

Water in Space *

The Water World of ISO

José Cernicharo

*CSIC. Instituto de Estructura de la Materia. Dpt. Molecular and Infrared Astrophysics.
C/Serrano 121. 28006 Madrid. Spain (cerni@damir.iem.csic.es)*

Jacques Crovisier

*Observatoire de Paris, 5 place Jules Janssen, F-92195 Meudon, France
(jacques.crovisier@obspm.fr)*

Abstract. In this review we present the main results obtained by the ISO satellite on the abundance and spatial distribution of water vapor in the direction of molecular clouds, evolved stars, galaxies, and in the bodies of our Solar System. We also discuss the modeling of H₂O and the difficulties found in the interpretation of the data, the need of collisional rates and the perspectives that future high angular and high spectral resolution observations of H₂O with the Herschel Space Observatory will open.

Keywords: water – molecular clouds – evolved stars – galaxies – comets – Mars – giant planets – Titan

Received: 8 April 2005, **Accepted:** 14 April 2005

1. Introduction

The determination of the abundance of water vapor is a long standing problem in astrophysics. Because water vapor is predicted to be an abundant molecule in the gas phase, a determination of its spatial extent, its distribution, and its abundance is crucial in modeling the chemistry and the physics of molecular clouds. In warm molecular clouds, water vapor could play a critical role in cooling the gas (Neufeld and Kaufman 1993, Neufeld et al., 1995) and, hence, in the evolution of these objects. In spite of the important astrophysical output that could be obtained from near, mid and far-infrared observations of water vapor (see, e.g., Cernicharo 1998; van Dishoeck 2004), the wavelength range 2-200 μm was poorly studied prior to ISO due to the large absorption at H₂O frequencies produced by water vapor in the Earth's atmosphere.

Some ground-based and airborne observations of H₂O have been performed, but most of the observed transitions are maser in nature making very difficult the analysis of the data (Waters et al., 1980, Cernicharo et al., 1990, 1994, 1996a; Menten and Melnick 1991; González-Alfonso et al.,

* Based on observations with ISO, an ESA project with instruments funded by ESA Member States (especially the PI countries: France, Germany, the Netherlands and the United Kingdom) and with the participation of ISAS and NASA.



1995, 1998a; Cernicharo et al., 1999). Even the observation of the H_2^{18}O isotope gives only poor estimates on $x(\text{H}_2\text{O})$ due to contamination of the observed transitions by other molecular lines (Jacq et al., 1988, Gensheimer et al., 1996), or to the observation of only one line which avoids the correct determination of the excitation conditions of the ^{18}O isotopic species of water vapor (Zmuidzinas et al., 1995). HDO has been also observed (see, e.g., Jacq et al., 1990; Helmich et al., 1996a; Pardo et al., 2001b; Comito et al., 2003), but it is also difficult to derive the H_2O abundance from this rare isotopic species. Some efforts have been made as well to derive the water abundance in molecular clouds from the observation of related species like H_3O^+ (Phillips et al., 1992; Goicoechea & Cernicharo 2001a). However, the determination of the H_2O abundance from these observations is not straightforward.

The $6_{16}-5_{23}$ masing transition of H_2O at 22 GHz, which arises from levels around 700 K, has been used since its detection by Cheung et al., (1969), to trace high excitation gas around star forming regions and evolved stars. The size of the emitting regions at this frequency is typically of the order of a few milliarcseconds (a few 10^{13} cm at the distance of Orion). Hence, no information has been obtained on the role of water vapor at large spatial scales from this line. Other H_2O lines have been detected from ground or airborne based telescopes like the $3_{13}-2_{20}$ transition at 183 GHz (Waters et al., 1980; Cernicharo et al., 1990, 1994, 1996a; González-Alfonso et al., 1995, 1998a), the $4_{14}-3_{21}$ transition at 380 GHz (Phillips, Kwan and Huggins 1980), the $10_{29}-9_{36}$ transition at 321 GHz (Menten, Melnick and Phillips 1990a) and the $5_{15}-4_{22}$ transition at 325 GHz (Menten et al., 1990b; Cernicharo et al., 1999). Among these lines only the $3_{13}-2_{20}$ transition at 183 GHz, for which the terrestrial atmosphere can be partially transparent under excellent weather conditions (see Cernicharo 1985, 1988; Cernicharo et al., 1990; Pardo 1996, Pardo et al., 2001a for details on atmospheric transmission at mm and submm wavelengths), has been used to map the emission of water at very large spatial scales (Cernicharo et al., 1994, 1996a, 1997b,c). As an example, the map of the Orion molecular cloud shown in Cernicharo et al., (1994) is 6 orders of magnitude larger than the size of the spots detected at 22 GHz. In that work the water abundance was estimated for the different large scale components of the Orion molecular cloud for the first time. However, due to the maser nature (although relatively weak) of this water transition, the interpretation of the data depends critically on the assumed kinetic temperature of the gas. In Orion, Cernicharo et al., (1994) estimate that changing the temperature of the emitting gas from 60 K (the assumed value) to 150 K the water abundance required to fit the data would be reduced by one order of magnitude in the extended ridge molecular cloud.

The ISO mission (Kessler et al., 1996), and especially, the *Long Wavelength Spectrometer*, LWS (Clegg et al., 1996), and the *Short Wavelength Spectrometer*, SWS (de Graauw et al., 1996), have provided a unique op-

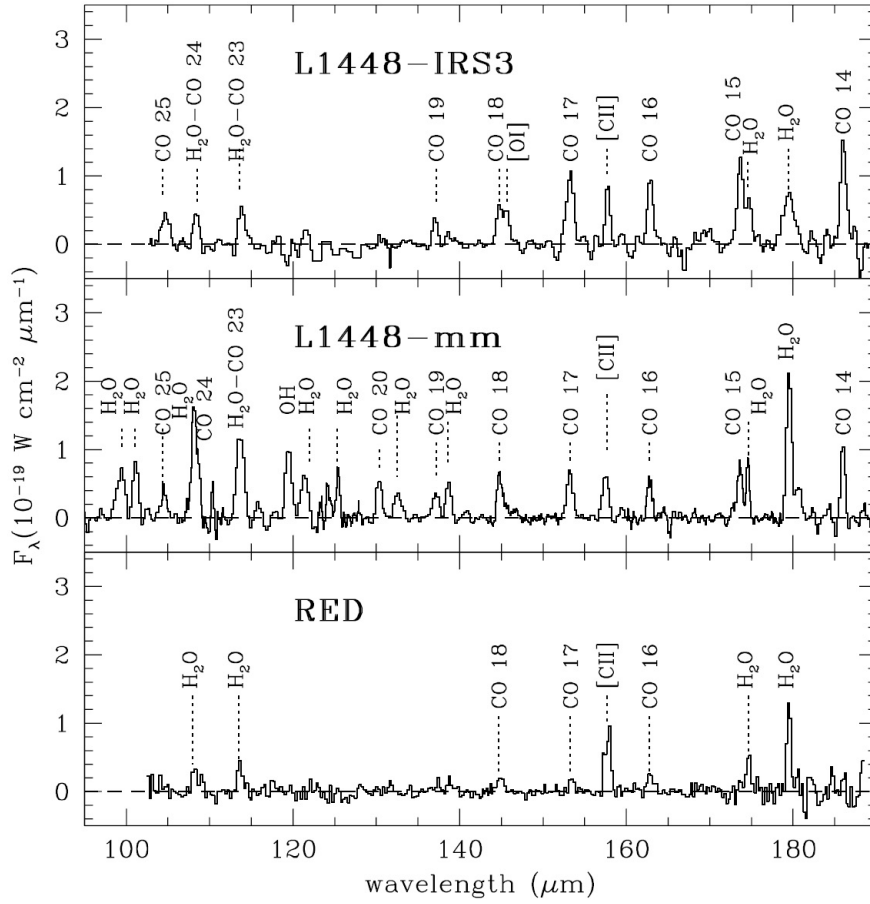


Figure 1. ISO/LWS continuum-subtracted spectra in the direction of L1448-IRS3 and L1448-mm and the red lobe of the outflow associated to L1448-mm. The lines from OH, H₂O and CO, together with atomic fine structure lines, are indicated in the different panels (from Nisini et al., 2000).

portunity to observe several H₂O lines in a large variety of astronomical environments. The SWS spectrometer covers the region 2-45 μm and is well adapted to study ro-vibrational transitions (stretching and bending modes). On the other hand, the LWS spectrometer provides a powerful tool to observe the pure rotational transitions of light molecular species like H₂O. The majority of the observations of H₂O pure rotational lines were performed at the low spectral resolution of the LWS grating mode ($\sim 1000 \text{ km s}^{-1}$), which produces strong spectral dilution in the search for molecular features in most ISM sources. Nevertheless, some molecular clouds, such as Orion and SgrB2, have been observed in many water lines using the much higher resolution of

the Fabry-Pérot coupled to the SWS and LWS instruments ($\sim 10 \text{ km s}^{-1}$ for the SWS/FP and $\sim 35 \text{ km s}^{-1}$ for the LWS/FP; see Figures 2 & 3).

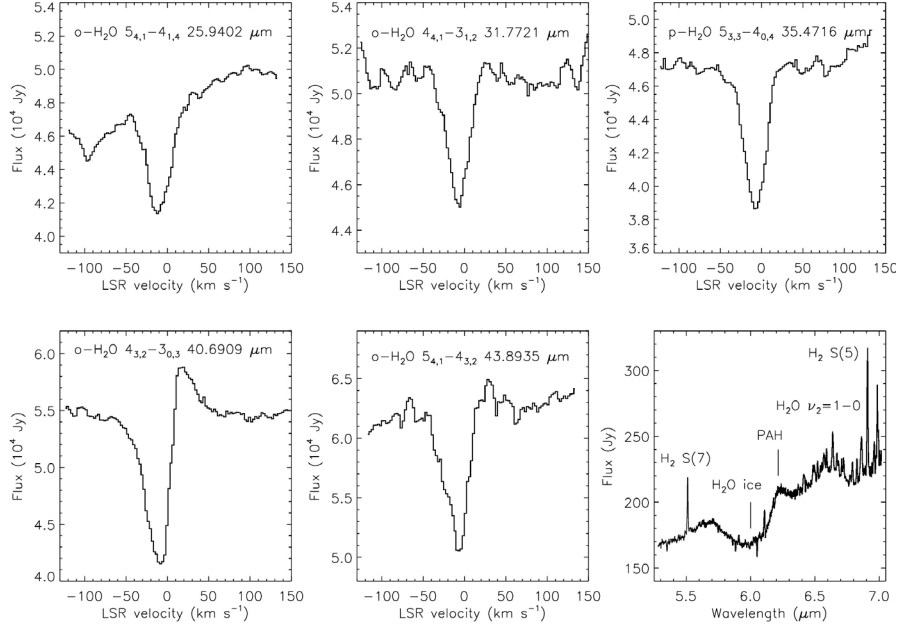


Figure 2. SWS Fabry-Perot spectra toward IRC2 of a selection of H_2O absorption lines. The final panel displays the 5.3-7.0 μm grating spectrum of the $\text{H}_2\text{O } \nu_2=0 \rightarrow 1$ (see section 2.2 for the analysis of this feature; from Wright et al., 2000).

The instruments on board the Infrared Space Observatory (ISO) have provided the most complete opportunity to study the emission/absorption of water and other important molecular species through transitions which are inaccessible from the ground or airborne platforms. Other space observatories, like Odin (see Hjalmarsen et al., 2003), and the *Submillimeter Wave Astronomy Satellite* (SWAS; Melnick et al., 2000), have also provided data on the ground transition of *o*- H_2O at 557 GHz. These two satellites provide a higher spectral resolution than ISO, with the drawback of having access to only one line of water vapor and a lower angular resolution. The higher angular resolution provided by ISO and the possibility to cover the full 2-200 μm range, i.e., the pure rotational spectrum of H_2O and the ro-vibrational transitions associated to its bending and stretching modes, makes ISO the most powerful instrument available so far for the study of water vapor. In this review we present the main results on gas phase H_2O obtained with the ISO-SWS and ISO-LWS spectrometers in the direction of molecular clouds, evolved stars, galaxies and solar system bodies.

2. Water in the ISM

ISO has provided observations of H₂O in a large variety of objects of the ISM (see, e.g., van Dishoeck 2004 for a review on ISO spectroscopy). The low spectral resolution data from the LWS have been used to study the water emission in shocks, photo dissociation regions, and high and low mass protostars.

Fig. 1 shows the far-infrared spectrum at several positions of the class 0 source L1448 (Nisini et al., 2000). These data show the presence of H₂O, OH, CO and atomic fine structure lines. The far infrared cooling is mainly due to the emission of these species, together with H₂ in the mid and near infrared. The ISO observations probe a gas of very different physical conditions to those determined from ground based telescopes. The water molecules and H₂ seem to be excited to temperatures between 500 and 1200 K. Probably this emission arises from very thin layers of shocked gas along the jet emerging from L1448-mm. In spite of the low spectral resolution of the LWS grating spectrometer, the sensitivity of ISO allows to study this gas in detail. The low and medium-J lines of CO that have been observed from ground based observatories trace a colder gas arising from different regions of the shocks.

The number of low mass protostars studied with the LWS is rather impressive. In most cases the observed water emission has been interpreted as arising from shocks along the molecular jet (see above for L1448; Moro-Martín et al. 2001, for CepE; Ceccarelli et al., 1999a, for IRAS16293-2422; Nisini et al., 1996, and Liseau et al., 1996, for HH54; Benedettini et al., 2000, for HH24-26; etc., see the review by Nisini 2003, and Nisini, Giannini and Lorenzetti 2002). Water vapor emission was also found in the direction of IC1396N, a bright rimmed globule, by Saraceno et al., (1996).

The LWS water emission measured toward young low mass stars have been also interpreted, using sophisticated models, as arising from the envelopes that surround the protostars (see, e.g., Ceccarelli et al., 1999b). Maret et al., (2002) have modeled the water, CO and OH lines in the far-infrared in the direction of NGC1333-IRAS4 and conclude that the observed emission is reasonably well reproduced by their models. However, the lack of angular resolution and the poor sensitivity of most water lines to the physical parameters, avoid a clear assignment of the observed emission to the very small regions surrounding the newly formed protostars. Herschel will provide a more detailed view of the origin of water vapor in these objects. Nevertheless, the 183.3 GHz observations of water by Cernicharo et al., (1996a) toward HH7-11 and L1448 seem to indicate that H₂O is present in both the shocks along the molecular jets and the central source.

High spectral resolution (from 7-40 km s⁻¹) with ISO is available for just a few molecular clouds. The SWS/FP instrument has been used mainly to observe the bending mode of water in the direction of high mass protostars

and to observe pure rotational lines of H_2O in Orion (see, e.g., Wright et al., 2000). The LWS/FP has been used to observe pure rotational lines of water in a large variety of molecular clouds. Fig. 3 shows the LWS/FP results in the direction of Sgr B2(M). Lines from OH, H_2O , C_3 , NH, NH_2 , NH_3 , CH, HD, and CH_2 and atomic fine structure features have been detected (Cernicharo, Goicoechea and Caux 2000; Goicoechea and Cernicharo 2001ab, 2002; Goicoechea, Rodríguez-Fernández and Cernicharo 2004; Ceccarelli et al., 2002; Polehampton et al., 2002, 2005). These observations provide a spectral resolution of $\simeq 35 \text{ km s}^{-1}$, which is enough to probe molecular clouds with broad lines, but precludes the study of more quiescent clouds with narrow lines. The Herschel Space Observatory will get around this problem thanks to its high spectral resolution heterodyne receiver HIFI. Relevant observations of water with the SWS/FP instrument have been reported by Wright et al., (2000, see Figure 2).

Water ice has been observed toward a large number of molecular clouds. Gibb et al., (2004) give an overview of the stretching and bending water ice features in clouds of the ISM. The review by van Dishoeck (2004) provides a detailed view on the gas and ice spectroscopy that ISO has performed.

We are going to present in more detail selected ISO data on prototypical ISM objects such as Orion, SgrB2 and cold dark clouds. The goals are to show how different the water line profiles could be depending on the physical conditions of the cloud, the difficulties in getting physical parameters (a benchmarking of radiative transfer codes for water vapor was held in 2004 at the Lorentz Center in Leiden; van der Tak et al., 2005), and the need to carefully select the water lines we could wish to observe with future space observatories, like Herschel, in order to have a correct view of the excitation conditions of water and to get a good estimate of the physical conditions of the clouds.

2.1. THE PURE ROTATIONAL LINES OF WATER

2.1.1. *Rotational Water Vapor Lines in Emission : Orion*

The Orion Kleinmann-Low nebula (Orion-KL) is the nearest (at a distance of $\sim 450 \text{ pc}$) and probably the most studied star forming region in the sky (see e.g., Genzel and Stutzki review 1989). The core of Orion-KL is associated with several places of massive star formation, and thus, the cloud is heavily influenced at large scales by violent phenomena such as outflows and shocks. The brightest objects are BN and IRC2, which are separated $\leq 10'$. Among these sources, IRC2 has the largest intrinsic luminosity ($L \sim 10^5 L_\odot$). The fact that multiple gas components with different physical conditions and velocity fields overlap along the line of sight complicates the interpretation of data from Orion-KL. This also results in a segregation of the gas and dust chem-

istry: different species and different reaction patterns dominate in the different regions (e.g. Blake et al., 1987).

Many molecular observations from the millimeter to IR domains have contributed to the characterization of the three main gas components towards Orion IRC2. The *Hot Core*, centered $\sim 2''$ south of IRC2 with a diameter of $\sim 10''$ is probably an ensemble of warm and dense ($\leq 10^7 \text{ cm}^{-3}$) clumps. Spectral lines arising from the hot core show line widths of $\Delta v = 5\text{--}15 \text{ km s}^{-1}$ at $v_{LSR} \simeq 6 \text{ km s}^{-1}$. The *outflows* or the *plateau*, with a diameter of $\leq 40''$, give a highly anisotropic emission from gas flows at high- ($\sim 100 \text{ km s}^{-1}$) and low-velocity ($\sim 18 \text{ km s}^{-1}$) with $\Delta v = 30\text{--}150 \text{ km s}^{-1}$ and centered $v_{LSR} \simeq 9 \text{ km s}^{-1}$. These flows encounter inhomogeneous density media in their way out, producing shocked regions, and finally plunge into the extended cloud. In particular, shocks produced by the interaction of the high velocity flow and the surrounding cloud at $\sim 30\text{--}40''$ from IRC2, produce the bright H_2 regions known as Peak1 and Peak2 (first detected by Beckwith et al., 1978). Finally the whole region is embedded in a quiescent and extended component (the molecular *Ridge*) with narrow line-widths $\Delta v = 3\text{--}5 \text{ km s}^{-1}$. All these inhomogeneous components are spatially present in the ISO LWS and SWS beams and may thus contribute to the emerging mid- and far-IR spectrum of water vapor.

Several ground-based observations of water maser lines have been performed in the Orion-KL region. From VLBI observations of the $\text{o-H}_2\text{O}$ line at $\sim 22 \text{ GHz}$, Genzel et al., (1981) determined the kinematics and velocity of the 18 km s^{-1} flow while the widespread nature of the water vapor around IRC2 has been probed with maps of water at $\sim 183 \text{ GHz}$ (Cernicharo et al., 1990; 1994). This was the first time that water vapor was detected, and its abundance estimated, in the different large scale components of Orion IRC2. In addition, the high excitation of the plateau gas has also been revealed by observations of water at $\sim 325 \text{ GHz}$ (Menten et al., 1990b; Cernicharo et al. 1999). Still, the interpretation of the excitation mechanisms of these maser lines is not obvious. The HDO species has also been detected and modeled towards Orion (Jacq et al., 1990; Pardo et al., 2001b), but is not straightforward to obtain water abundances without taking into account the chemistry of each gas component. ISO spectrometers have provided the unique opportunity of observing many IR thermal lines towards Orion.

Fig. 4 shows the LWS data in the direction of Orion. Several positions were observed between 45 and $198 \mu\text{m}$ providing information on atomic fine structure lines as well as on CO and H_2O pure rotational lines (see Sempere et al., 2000 for an analysis of the CO data). This Figure shows that water vapor is present over a region of several arcminutes in size (see also the 183.3 GHz observations of Cernicharo et al., 1994). The intensity of the water lines decreases from the center to the surrounding positions by a factor of 10, which corresponds to a variation in both the water abundance and the physical

conditions of the gas. The large spatial distribution of water emission makes extremely difficult the interpretation of the water lines. In addition, this large scale map has been obtained in the grating mode of the LWS spectrometer, i.e., with a spectral resolution of 300-600. Hence, no information is available on line profiles.

Harwit et al., (1998) have published the results on 8 lines of water observed with the LWS/FP between 71 and 125 μm (see Fig. 5) and conclude that these lines arise from a molecular cloud subjected to a magnetohydrodynamic C-type shock. The lines indicate a water abundance of the order of $5 \cdot 10^{-4}$. However, the fine interpretation of these lines is not obvious as radiative pumping from IR photons could be playing an important role in the excitation of water. Moreover, the collisional rates for the temperatures prevailing in the shock are poorly known. One will need a larger set of lines, including those from the isotopic species of water. Some additional lines were observed with the ISO/SWS/FP spectrometer by Wright et al., (2000; see Fig. 2). Opposite to the long wavelength water line profiles, the lines appear in absorption below 40 μm . The authors have obtained a water abundance of $2\text{-}5 \cdot 10^{-4}$ for a kinetic temperature of 200-350 K in the warm shocked gas. The turnover point between absorption and emission is an important clue in interpreting the data (opacity, line strength, spatial distribution of the gas,...). Cernicharo and co-workers have observed all water lines in the LWS domain with the FP including several lines of the isotopic species H_2^{18}O and H_2^{17}O . In addition, they have made a map with the LWS/FP in two water lines in order to constrain the models of the different excitation processes of water. These authors have detected more than 60 pure rotational thermal lines with the LWS Fabry-Pérot on board ISO, including also several lines of the H_2^{18}O and H_2^{17}O isotopologues of H_2O . Fig. 6 shows a selection of the observed lines together with the low resolution spectrum of Orion.

Water lines with upper energy levels below ~ 1500 K have been detected by ISO towards Orion IRc2. Nevertheless, the spatial/spectral resolution of these thermal water IR lines is not enough to resolve the complexity of the observed regions. As an example, it is difficult to separate narrow from broad water line components or to have the sensitivity to trace the line-wing emission. Besides, several radiative transfer effects (e.g., self-absorption and scattering) may possibly occur at velocity scales that cannot be resolved by ISO.

Due to the complexity of the region and the different excitation conditions prevailing along the line of sight, many water lines have to be taken into account in the models. The H_2^{16}O lines with wavelengths above $100\mu\text{m}$ are seen in emission. However for shorter wavelengths, lines arising from energy levels below $\sim 700\text{K}$ and with large line strengths show P-Cygni profiles and have a large emission/absorption velocity range, while those with weak line strengths, or arising from higher energy levels, are observed in pure emission. Note that most water lines detected by ISO below $\sim 45 \mu\text{m}$ (van Dishoeck et

al., 1998; Wright et al., 2000) are observed in pure absorption. The peak LSR velocity of the emission lines occurs around $+20 \text{ km s}^{-1}$, while that of pure absorption lines occurs at -8 km s^{-1} (Wright et al., 2000). This means that the filling factors for water vapor as seen by the LWS and SWS beam apertures are different, i.e., the water emission observed by LWS-FP is likely arising from a larger surface than that observed with the SWS-FP. In fact, the far-IR thermal emission in the water line at ~ 179.5 and $\sim 174.6 \mu\text{m}$ respectively, is clearly more extended than the cloud position represented by Orion IRc2 (Cernicharo et al., 2005). The widths of the far-IR water lines are broader than the instrumental width determined by the Lorentzian instrument response, thus, the water lines are partially resolved.

The angular extent and the spatial origin of the far-IR water lines is the main drawback when trying to model the spatially unresolved ISO observations. Besides, any detailed fit to the data requires a detailed knowledge of the geometry and of the relative distribution of dust and water. Fortunately, the high angular resolution maps of water obtained from ground-based observations of the 183.3 and 325 GHz lines do reveal the spatial and velocity distribution of water vapor (Cernicharo et al., 1994; 1999). These authors detected at least four different water components from which the millimeter and submillimeter water lines arise: the extended molecular Ridge, the high-velocity outflow, the low-velocity outflow and very narrow and strong features which are also associated with the small bullets observed at 22GHz (Genzel et al., 1981).

The interpretation of these lines requires detailed non-LTE and non-local statistical equilibrium calculations and radiative transfer models including both gas and dust (Daniel, Goicoechea & Cernicharo 2005). Fig. 7 shows these models (including gas and dust) for different water vapor abundances. The original code has been described in detail by González-Alfonso & Cernicharo (1993, 1997, 1999). Models assume that most of the water emission/absorption arise from the low-velocity Plateau, although the effect of the lower excitation extended Ridge has also been investigated. A spherical geometry for an outflow expanding at 18 km s^{-1} consisting of two cloud components of different temperatures and densities has been adopted. These gas and dust layers surround a $10'$ continuum IR source (the hot core), with color temperatures between 200 and 300K. The effect of this continuum radiation and the effect of the dust opacity, together with collisions, has a deep impact in the population of H_2O rotational levels (Cernicharo et al., 2005; Daniel, Goicoechea & Cernicharo 2005). The models reproduce quantitatively and qualitatively the observed profiles and intensities of the water lines and the IR continuum detected by ISO. However, some water vapor lines are sensitive to the water abundance while other are sensitive to the adopted geometry. Very high abundances, $3 \cdot 10^{-4}$, are needed to explain most lines below $40 \mu\text{m}$, while abundances between $3 \cdot 10^{-5}$ to 10^{-4} are required for the long

wavelength lines. In addition, some lines are difficult to be reproduced by the models. Calibration errors and/or inaccuracy in the collisional rates could be responsible for these effects. The water abundance, as derived from ISO and ground based observations, is consistent with that derived by Wright et al., (2000) and Harwit et al., (1998), a few 10^{-4} for the shocked regions, and decreases to 10^{-5} - 10^{-6} for the large scale components. Any realistic model of water for clouds such as Orion has to properly take into account the phenomena described above. The high angular and spectral resolution that will be provided by Herschel will allow us to improve the models for water vapor in Orion.

2.1.2. Rotational Water Vapor Lines in absorption : Sgr B2

Sgr B2 is the most massive cloud in the Galaxy, $\sim 10^7 M_{\odot}$ (Lis and Goldsmith 1990). This cloud is a paradigmatic object in the Galactic Center region as its geometrical properties, physical conditions and chemical characteristics resemble a miniature galactic nucleus with a $\sim 15'$ extend (Goicoechea et al., 2004). Opposite to what is found toward other star forming regions, such as Orion (see above and Cernicharo et al., 1998a), the observations of the $2_{12} - 1_{01}$ line at $\sim 179.5 \mu\text{m}$ in the direction of Sgr B2 show that the line appears in absorption rather than in emission (Cernicharo et al., 1997a). Later, the launch of SWAS allowed the observation of the $1_{10} - 1_{01}$ fundamental transition of both H_2^{16}O at 557 and H_2^{18}O at 548 GHz (first detected by the *Kuiper Airborne Observatory*, KAO; see Zmuidzinas et al., 1995). Although the velocity resolution is $\sim 1 \text{ km s}^{-1}$, the large beam of SWAS ($\sim 4'$) could make these observations mostly sensitive to the extended cold and less dense gas. SWAS observations have provided an estimate of the H_2O abundance in the low excitation clouds located in the line of sight toward Sgr B2 (Neufeld et al., 2000, 2003). However, the fact that only the ground-state absorption line is detected makes difficult a detailed study of the water vapor excitation mechanisms in Sgr B2. Cernicharo et al., (2005) get around this problem with their analysis of the far-IR observations of 14 thermal lines of water vapor toward Sgr B2(M) with the ISO/LWS/FP spectrometer, and the first mapping of the 183.3 GHz maser emission of para- H_2O around Sgr B2 main condensations.

The far-IR spectrum of Sgr B2(M) is dominated by the absorption produced by H_2O , NH_3 , C_3 , OH , and NH (see Cernicharo et al. 1997a, 2000; Ceccarelli et al., 2002, Goicoechea et al., 2001b, 2004). The low resolution spectrum obtained with the LWS, together with the available data from the LWS/FP, have been analyzed by Goicoechea et al., (2004; see Fig. 21 for a comparison of the grating spectrum of Sgr B2(M) and Arp220). The dust emission could be fitted with a $T_{dust} \simeq 30 - 40 \text{ K}$ with a peak opacity at $80 \mu\text{m}$ of $\simeq 5$. A detailed view of the absorption lines found in SgrB2 in the $40 - 200 \mu\text{m}$ range is shown in Fig. 3 while those of water vapor are shown in Fig. 8.

Except the $2_{12} - 1_{01}$ ground state line at $\sim 179.5 \mu\text{m}$, all water lines have the same profile and are centered at Sgr B2(M) velocities. The $\sim 179.5 \mu\text{m}$ line appears saturated and in absorption from -150 to $+100 \text{ km s}^{-1}$ indicating that is tracing both cold water vapor located in the foreground gas toward the GC and the warm gas around Sgr B2(M). The widespread absorption produced by the $2_{12} - 1_{01}$ line has been previously presented by Cernicharo et al., (1997a), while the $1_{10} - 1_{01}$ absorption has been mapped with SWAS (Neufeld et al., 2003). These observations probe that low excitation H_2O is present in the clouds along the line of sight of Sgr B2. The averaged velocity from all H_2O lines observed with the ISO/LWS-FP is $+50 \pm 5 \text{ km s}^{-1}$, in agreement with the velocity of other related O-bearing species such as H_3O^+ or OH (Goicoechea & Cernicharo, 2001a; 2002). Taking into account the wavelength calibration accuracy of the LWS/FP instrument, this velocity is in reasonable agreement with the expected $+65 \text{ km s}^{-1}$ cloud seen in radio observations (Hüttemeister et al., 1995). Note, however, that velocities close to $+50 \text{ km s}^{-1}$ are also associated with gas surrounding most of the Sgr B2 continuum sources, so that the bulk of the H_2O absorption can arise from this specific LSR component (note also that the 183.3 GHz line appears in some positions at this velocity; see Fig. 9). Possible overlaps with other molecular species occur at some wavelengths. In particular, the o- H_2O $4_{32} - 4_{23}$ line is blended with HF $J=2-1$ at $121.697 \mu\text{m}$ (Neufeld et al., 1997) and the o- H_2^{18}O $2_{12} - 1_{01}$ line at $181.053 \mu\text{m}$ has a small contribution from the H_3O^+ Q(1,1) line (Goicoechea & Cernicharo 2001a).

Observations of the H_2O $3_{13} - 2_{20}$ line ($E_l \simeq 200 \text{ K}$) at $\sim 183 \text{ GHz}$ toward Sgr B2 are presented in Fig. 9 (integrated line intensity over the observed region and several spectra at relevant positions). The emission appears at the LSR velocities of Sgr B2 with no contribution from other clouds along the line of sight. Note the different line shapes and intensities of the $\sim 183 \text{ GHz}$ emission for positions in front and around the main condensations.

Different models (LVG and non-local) for the water vapor absorption have been presented in Cernicharo et al., (2005). The authors conclude that the LVG method is not well suited to treat the radiative transfer of H_2O in Sgr B2. To take into account the radiative coupling between regions with different physical and/or excitation conditions, the RT has to be treated with nonlocal techniques. In order to constrain the physical parameters they have used the available spectroscopic ground based and ISO data of CO and other species, including the extended maser emission from H_2O at 183.3 GHz. The models include all the rotational levels of H_2O involving transitions with wavelengths longer than $40 \mu\text{m}$. The level population is computed considering collisional excitation and radiative excitation by line and continuum photons emitted by the dust. This has been computed consistently assuming that the water molecules and the dust grains are coexistent. The geometry is a core+shell structure. Obviously all water transitions in the core are thermalized to the

dust temperature due to the large opacity in the far-IR. The computed line profiles are a result of convolving with the angular resolution of the LWS detectors ($\sim 80''$). To test the sensitivity of the models against the physical parameters, $N(\text{H}_2\text{O})$ and T_k were computed for 1.8×10^{16} , 9×10^{17} and $1.8 \times 10^{18} \text{ cm}^{-2}$, and 40, 100, 200, 300 and 500 K respectively, while densities were explored in the range from 5×10^3 to $6.4 \times 10^5 \text{ cm}^{-3}$ by steps of 2. The different non-local models for $N(\text{H}_2\text{O}) = 9 \times 10^{17} \text{ cm}^{-2}$ are shown in Fig. 10.

The main problem to interpret the H_2O absorption toward Sgr B2 is due to the large opacities of the far-IR water lines, typically $\sim 10^3$ and even $\sim 10^4$ for the ortho- H_2O $2_{12}-1_{01}$ line at $\sim 179.5 \mu\text{m}$. Under these conditions, many weak water lines have to be detected in order to constrain the physical conditions and the column density. In addition, as the radiative excitation dominates the population of the far-IR levels, lines with a weak dependence on the dust excitation should be searched. Taking into account the 14 water lines detected in the far-IR, the nonlocal results imply that these lines are not very sensitive to the temperature and that the only indication about the column density has to be searched in weak far-IR H_2O lines or in the 183.3 GHz one. Even so, the far-IR absorption arises from the low density external layers of gas, while it is very likely that the 183.3 GHz line could have an important contribution from inner and denser regions. Another problem arises from the fact that models with low $N(\text{H}_2\text{O})$ values and $T_k \lesssim 200 \text{ K}$, indicated that it is also difficult to distinguish between different H_2 densities. Limits to T_k and $n(\text{H}_2)$ have to be searched in weak lines below $70 \mu\text{m}$.

The models for high water column densities (Fig. 10) predict absorption lines in the LWS range at ~ 56.3 , ~ 57.6 , ~ 58.7 , ~ 78.7 , ~ 99.5 , ~ 125.4 and $\sim 136.5 \mu\text{m}$. At the spectral resolution and sensitivity of the LWS/FP, none of these lines can be detected (and they have not). This implies $N(\text{H}_2\text{O}) < 10^{18} \text{ cm}^{-2}$ toward the warm envelope of Sgr B2. The $\sim 136.5 \mu\text{m}$ line, also predicted by the models with large $N(\text{H}_2\text{O})$, is contaminated by the absorption produced by the C_3 $Q(8)$ ro-vibrational line, which is also predicted by the models for tri-atomic carbon absorption in Sgr B2 (Cernicharo et al., 2000).

In addition, Cernicharo et al., (2005) have not detected any line of water vapor at wavelengths shorter than $60 \mu\text{m}$. Some of these lines are predicted (even in emission) by the models with large $N(\text{H}_2\text{O})$. Models considering $N(\text{H}_2\text{O}) = 1.8 \times 10^{16} \text{ cm}^{-2}$ are compatible with ISO detections and non-detections. Only the $\sim 67.1 \mu\text{m}$ line is weaker than observed. Taking into account the difficulties related to the H_2O models in the far-IR, Cernicharo et al., (2005) conclude that $(4 \pm 2) \times 10^{16} \text{ cm}^{-2}$ is the best H_2O column density to fit the ISO observations of the gas surrounding Sgr B2.

The array of models in Fig. 10 shows the difficulty in interpreting the far-IR data for H_2O . However, such variety of models has to be computed in order to test the sensitivity of the water lines to the physical parameters and to

collisional and/or radiative pumping. Future observations with the Herschel Space Observatory will provide data at high angular resolution, similar in fact to that achieved in ground based 183.3 GHz observations. However, the correct selection of the water lines sample to be observed will be critical to interpret the data and to derive the physical conditions of the gas and the water abundance.

2.1.3. *Water Vapor Lines in absorption : Dark Clouds toward Sgr A*

The abundance of water vapor in dark clouds has been analyzed through emission observations by SWAS (see, e.g., Snell et al., 2000). The upper limits they have obtained, $x(\text{H}_2\text{O}) \leq 7 \cdot 10^{-8}$, correspond to very low H_2O abundances and indicate that getting positive results when searching for water emission in very low kinetic temperature regions is difficult. Although some weak emission from such cold clouds could be expected, one has to take into account that the surrounding gas, even if the density is not enough to pump the rotational levels of H_2O , will absorb and re-emit over a large volume the photons arising from the densest regions in the cores of these clouds (see Cernicharo and Guélin 1987 for an analysis of this effect in the high dipole moment molecule HCO^+). The result is that extremely weak emission could arise from dark clouds. Consequently, emission measurements are not well suited to derive the abundance of H_2O . However, absorption measurements are better suited for this task in these objects when a continuum background source is available. Moneti, Cernicharo and Pardo (2000) have used ISO to derive the water abundance in the dark clouds in front of the galactic center Sgr A*. By observing CO and H_2O gas and ice features with the SWS and LWS spectrometers (see Fig. 11) they have been able to characterize the different components in the spectra : the warm gas surrounding Sgr A*, and the cold gas and dust in the dark clouds in front of this cloud. However, water line observations are not enough to constrain the physical properties of the gas. Therefore, they complemented their study with an analysis of the pure rotational high-J lines of CO, also observed by ISO, to provide some additional key parameters for the interpretation of the water lines (see Fig. 12). The use of the ro-vibrational and rotational lines of H_2O , which have very different opacities, and the information provided by other molecular species has been extremely useful in deriving the water abundance in dark clouds.

Plume et al., (2004), and references therein, have used the SWAS satellite to observe water absorption produced by the clouds placed in the line of sight toward W49A. They have derived H_2O abundances of $8.2 \cdot 10^{-8}$ to $1.5 \cdot 10^{-6}$, i.e., very similar values to those obtained in the dark clouds observed by Moneti, Cernicharo and Pardo (2000). Where these lines are formed, i.e., in the innermost regions of the cold clouds or in their external layers (photochemistry) is not clear yet. Future observations with the Herschel Space Observatory in several lines of water and its isotopic species (and other molecular

lines, like CO lines to constrain models and the interpretation of water emission/absorption) will provide a more detailed view of the water abundance and chemical processes leading to its formation in cold dark clouds.

2.2. THE BENDING MODE OF WATER

Helmich and collaborators (Helmich et al., 1996b) have detected many rovibrational lines of water vapor due to absorption from the ground level up to the bending mode, ν_2 , opening the way to study the role of water vapor in star forming regions. They detected more than 30 infrared absorption lines toward AFGL 2591 (see Fig. 13) arising from gas at high kinetic temperature, $T_K \simeq 300$ K. van Dishoeck and Helmich (1996) observed the bending mode of water toward massive young stars covering a large range of physical conditions. Hot water with excitation temperature >200 K was found toward GL 2136 and GL 4176 (in addition to GL 2591) with an abundance as large as $2\text{-}3 \cdot 10^{-5}$ and comparable to the abundance of H_2O in ices in the coldest parts of these clouds (see Fig. 13).

Boonman and van Dishoeck (2003) have analyzed the available observations of the bending mode of H_2O toward a significant number of molecular clouds and found water abundances in the range $5 \cdot 10^{-6} - 6 \cdot 10^{-5}$ with a clear tendency to have larger water abundances as the gas temperature increases, which suggests that grain-mantle evaporation is important. They have compared these results with chemical models showing that three different chemical processes, ice evaporation, high-T chemistry, and shocks, can reproduce the high gas-phase H_2O abundances inferred. Of course, the results concern the inner regions of the cloud that surrounds these massive protostars.

Although the observation of the bending mode of H_2O provides an excellent tool to derive water abundances in high mass star forming regions, the main drawback is that these observations are limited to the directions with strong infrared emission at $6 \mu\text{m}$, which are spatially limited to a few arcseconds. Nevertheless, the study of the bending mode of water could provide good insights on the role of infrared photons in pumping of water molecules to high energy levels. One of the nicest surprises provided by observations of the bending mode of H_2O with ISO occurred in Orion: Toward its central continuum source the R-branch of the band was observed in absorption while the P-branch was found in emission. These results were correctly interpreted by González-Alfonso et al., (1998b) and González-Alfonso and Cernicharo (1999; see Fig. 14; an overview of the H_2O ν_2 band is shown in the bottom-right panel of Fig. 2). In fact, theoretical models made for evolved stars predicted such a behavior under some specific physical and geometrical conditions (González-Alfonso and Cernicharo 1999). These models were done prior to the observations and the excellent agreement found provided strong confidence in the physical parameters obtained in the interpretation of the ro-

vibrational lines of water (high water abundances, the role of dust in the IR pumping, etc., see, e.g. González-Alfonso et al., 2002). Finally, the bending mode of water could also be observed in absorption in dark clouds when a strong infrared source is located behind the cloud (see section 2.1.3).

3. Water in Evolved Stars

3.1. O-RICH STARS

O-rich evolved stars, i.e., stars with $C/O < 1$, are the best water vapor factories in space. In the innermost layers of their circumstellar envelopes the physical conditions (high density and temperature) allow a chemistry under thermodynamical equilibrium. As CO is the most stable molecule in space, most carbon atoms are locked in CO leaving oxygen atoms available to build other gas phase species such as CO_2 and H_2O .

González-Alfonso and Cernicharo (1999) have modeled the water spectrum of evolved stars. The pure rotational lines and the bending mode were analyzed. Fig. 15 (left panel) shows these models for two different mass loss rate regimes. In the high end of mass loss rates, the far-infrared spectrum is fully dominated by the pure rotational lines of H_2O (the CO lines are also present but weaker than those of water). The low mass loss rate model in the same figure shows that CO and water lines have similar intensities but the densest water spectrum dominates the far-infrared emission. The models shown in Fig. 15 have been convolved to the spectral resolution of the LWS grating spectrometer and indicate that water will dominate all cooling processes in the envelope (at least in the regions where water is not yet photodissociated).

The predictions for the bending mode are rather surprising (Fig. 15, right panel). Depending on the mass loss rates, the size of the envelope, and the gas density (radiation versus collisions), the bending mode will present a peculiar behavior with the R-branch in absorption and the P-branch in emission for low mass loss rates (panel **b**), or with the P-branch in absorption/emission for high mass loss rates (panel **a**). Changing the size of the envelope has important effects on the shape of the bending band as shown in panel **c**, where some lines appear in absorption while other lines are in emission in each branch (see Figure caption). This kind of behavior was nicely verified in Orion (see above; González-Alfonso et al., 1998a; van Dishoeck et al., 1998) and shows that the observation of the whole bending band provides important constraints when modeling the water excitation.

The first ISO spectrum showing the pure rotational lines of H_2O was obtained by Barlow et al., (1996) in the direction of W Hya (see Fig. 16). The spectrum is dominated by a forest of water lines confirming that H_2O

molecules are the dominant coolants of the gas in the circumstellar envelope. They have found a water abundance of $8 \cdot 10^{-4}$ for $r \leq 4.5 \cdot 10^{14}$ cm and $3 \cdot 10^{-4}$ at large radii. The star mass loss rate is $6 \cdot 10^{-7} M_{\odot} \text{ yr}^{-1}$. Neufeld et al., (1996) also observed this object with the SWS/FP spectrometer. They obtained a mass loss rate of $(0.5 - 3) \cdot 10^{-5} M_{\odot} \text{ yr}^{-1}$, i.e., two orders of magnitude larger than the value obtained by Barlow et al., (1996) or that obtained from dynamical considerations. This difference is probably arising from the different physical parameters assumed in the interpretation and to the lack of precise collision rates for $\text{H}_2\text{O}-\text{H}_2$ at the temperatures prevailing in these warm objects. Justtanont et al., (2004) have analyzed all the available data for W Hya and conclude that the only way to put in agreement the mass loss rates calculated from different molecular tracers is to increase the water abundance. The best value they obtain from CO lines is $(3.5-8) \cdot 10^{-8} M_{\odot} \text{ yr}^{-1}$ which is a factor 10 below that of Barlow et al., (1996) and three orders of magnitude below the mass loss rate derived by Neufeld et al., (1996). The main drawback of water vapor observations in O-rich stars is the large line opacities through the whole envelope which make extremely difficult the selection of rotational lines sensitive to the physical conditions. Many other O-rich evolved stars have been observed with ISO. R Cas has been modeled by Truong-Bach et al., (1999) getting a water abundance of $1.1 \cdot 10^{-5}$. More detailed models have been developed to interpret the high mass loss rate stars VY CMa (Neufeld et al., 1999; they also report the detection of rotational lines inside the ν_2 level) and NML Cyg (Zubko et al., 2004).

Most AGB stars are bright in the mid infrared which favor the observation of the bending mode of water in these objects. However, the lack of spectral resolution with ISO makes difficult the interpretation of the data because low excitation lines form throughout the whole envelope while high excitation lines, showing probably P-Cygni profiles, arise from the innermost layers of the envelope. Justtanont et al., (1996) observed the ν_2 H_2O band toward NML Cyg (see Fig. 17). Although the column density of water they derive is high the excitation temperature is rather low implying that most lines in the SWS spectrum are formed in the external envelope. They also observed the ν_1 and ν_3 bands of H_2O at $2.7 \mu\text{m}$.

OH/IR objects are O-rich stars with a high mass loss rate. They are characterized by the presence of strong OH masers and strong emission in the infrared. ISO observed a large number of these objects with the LWS and SWS spectrometers. Sylvester et al., (1999) analyzed these data and found a wealth of broad spectral features due to crystalline silicates and crystalline water ice in emission and absorption. Crystalline ice at 43 and $60 \mu\text{m}$ was detected first toward these objects by Omont et al., (1990) using the Kuiper Airborne Observatory (KAO). The full frequency coverage of the SWS and LWS spectrometer permits a more detailed study of these bands. Sylvester et al., (1999) concluded that there is a certain onset value for the mass loss rate above

which these features appear in the spectrum. Water vapor is also present in the spectra of these objects (see Fig. 18). Molster et al., (2001, and references therein) have analyzed the ISO spectrum of NGC6302, one of the first objects observed with ISO showing the crystalline water ice bands. These bands have also been detected toward the C-rich planetary nebula CPD-568032 by Cohen et al., (1999).

3.2. C-RICH STARS

In carbon-rich stars $C/O > 1$ and all oxygen atoms will be locked into carbon monoxide. Hence, oxygen will be unavailable to build other molecules. Nevertheless, Melnick et al., (2001) have reported the detection of H_2O with SWAS in the direction of IRC+10216, the prototype of carbon-rich AGB stars. The far-IR spectrum of this object as observed by ISO was reported by Cernicharo et al., (1996b) and no clear indication of H_2O could be found as the spectrum is dominated by a forest of emission lines from CO and HCN. Melnick et al., (2001) have suggested that the observed water vapor is arising from the evaporation of cometary bodies orbiting IRC+10216. More sensitive observations with Herschel of several water lines having different excitation conditions could provide a clearer picture about the origin of H_2O in this star.

The situation is different for post-AGB carbon-rich stars. Herpin and Cernicharo (2000) have presented ISO LWS observations of the proto-planetary nebula CRL 618, a carbon rich object in a very fast evolutionary phase prior to reaching the planetary nebula stage. The far-infrared spectrum is essentially dominated by CO lines (see Fig. 19). All the other species have much lower intensities contrary to that found in the AGB star IRC+10216 where HCN lines (from the ground and vibrationally excited states) are as strong as those of CO (see Cernicharo et al., 1996b). The main difference between both objects has to be found in the physical structure of their CSEs. That of CRL 618 has a central hole in molecular species filled by a bright HII region.

In addition to the lines of CO, ^{13}CO , HCN and HNC, Herpin and Cernicharo (2000) reported the detection of H_2O and OH emission together with the fine structure lines of [O I] at 63 and 145 μm . The abundances of these species relative to CO are $4 \cdot 10^{-2}$, $8 \cdot 10^{-4}$ and $\simeq 4.5$ in the regions where they are produced. The authors have suggested that O-bearing species other than CO are produced in the innermost region of the circumstellar envelope. UV photons from the central star photodissociate most of the molecular species produced in the AGB phase and allow a chemistry dominated by standard ion-neutral and neutral-radical reactions. Not only these reactions allow the formation of O-bearing species but also modify the abundances of C-rich molecules like HCN and HNC for which the authors have found an abundance ratio of $\simeq 1$, much lower than what is typical in AGB stars. Herpin et al., (2002) have made a comparative study of three carbon-rich post-AGB

objects, CRL618, CRL2688 and NGC7027. In the early stages of the AGB to PN evolution (represented by CRL2688) the far-infrared spectrum is dominated by CO lines. In the intermediate stage, e.g., CRL618, very fast outflows are present which, together with the strong UV field from the central star, dissociate CO. The released atomic oxygen is seen via its atomic lines and allows the formation of new O-bearing species, such as H₂O, H₂CO and OH. At the planetary nebula stage, e.g., NGC7027, a large fraction of the old CO AGB material has been reprocessed. The far-infrared spectrum is dominated by atomic and ionic lines. New species, such as CH⁺ (see Cernicharo et al., 1997d), appear. The water vapor formed during the protoplanetary nebula stage has been photodissociated. The chemical evolution during the protoplanetary nebula stage has been modeled, using only neutral and neutral-radical reactions, by Cernicharo (2004). The radicals are the products of the photodissociation of molecules formed during the AGB phase of the star. The author has shown that H₂O, H₂CO (a molecule detected in CRL618 by Cernicharo et al., 1989), and CO₂ are easily formed in the warm and dense gas of the photodissociation region surrounding the hot central star. These models also predict very large abundances for other carbon chains and carbon clusters as those found by Cernicharo et al., (2001 a,b). Hence, photochemistry plays an important role in the chemical evolution of the envelopes of post-AGB stars making possible the presence of O-bearing species in a medium where the physical conditions and the atomic abundances would result in very little amounts of these species.

4. Water in Galaxies

Due to the small size of the ISO telescope the observation of water in gas phase toward extragalactic objects is strongly limited in sensitivity. Nevertheless, observation of water ice in 18 galaxies, from a sample of 103 galaxies observed with ISO, has been reported by Spoon et al., (2002). They have found that water ice is present in most ULIRGs, whereas it is weak or absent in the large majority of Seyferts and starburst galaxies.

Only a few objects show gas phase molecular emission or absorption : Arp220, NGC1064 and NGC253. Goicoechea, Martin-Pintado and Cernicharo (2005), have analyzed the OH emission/absorption in NGC1064 and NGC253, while Arp220 has been studied in detail by González-Alfonso et al., (2004). Fig. 20 shows the far-IR spectrum of Arp220 as observed by ISO. The spectrum looks very similar to that of Sgr B2 (see Fig. 21). The modeling of the Arp220 far infrared spectrum (see below), and of the OH lines in NGC1064 and NGC253, was done by comparison of their spectra with that of some well-studied Galactic sources, which provides important clues about the physical conditions in the regions where the lines are formed.

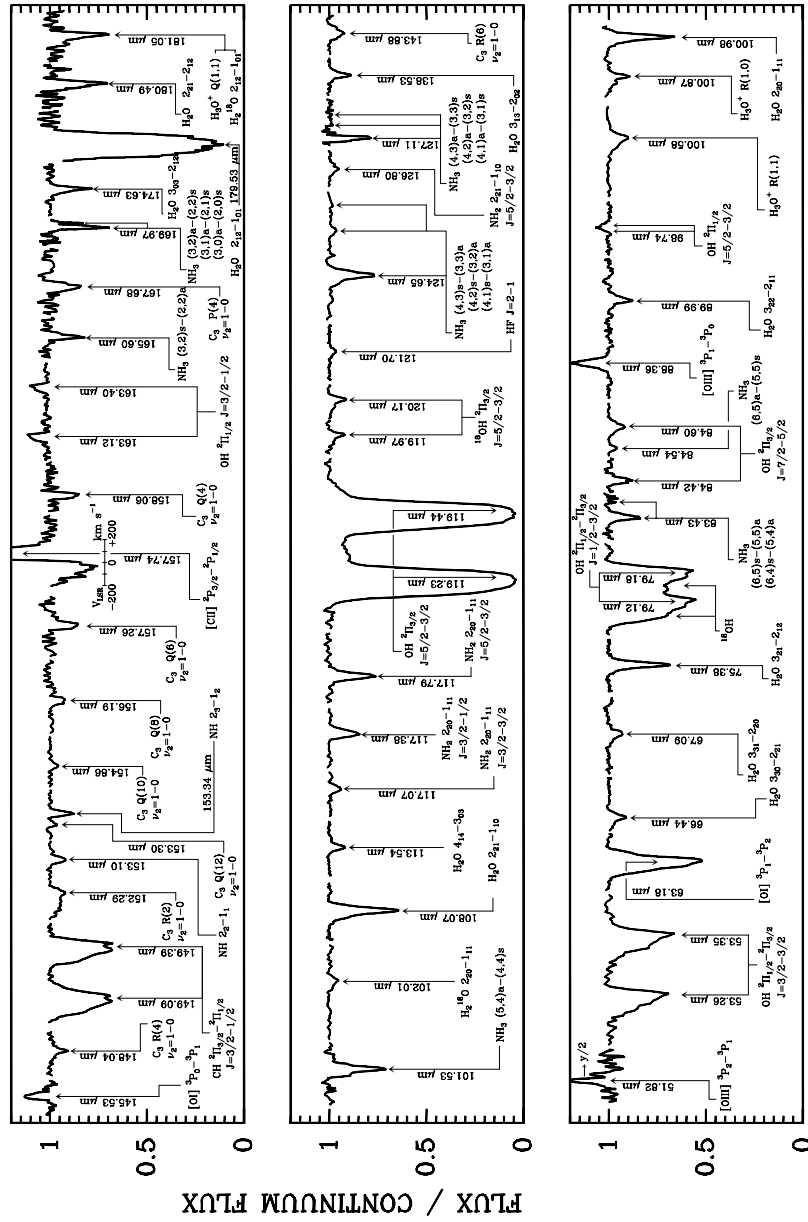


Figure 3. ISO/LWS/FP observations of Sgr B2(M). The lines from OH, H₂O, C₃, H₃O⁺, CH, NH, NH₂, and NH₃ and atomic fine structure lines are indicated from Goicoechea et al., (2004).

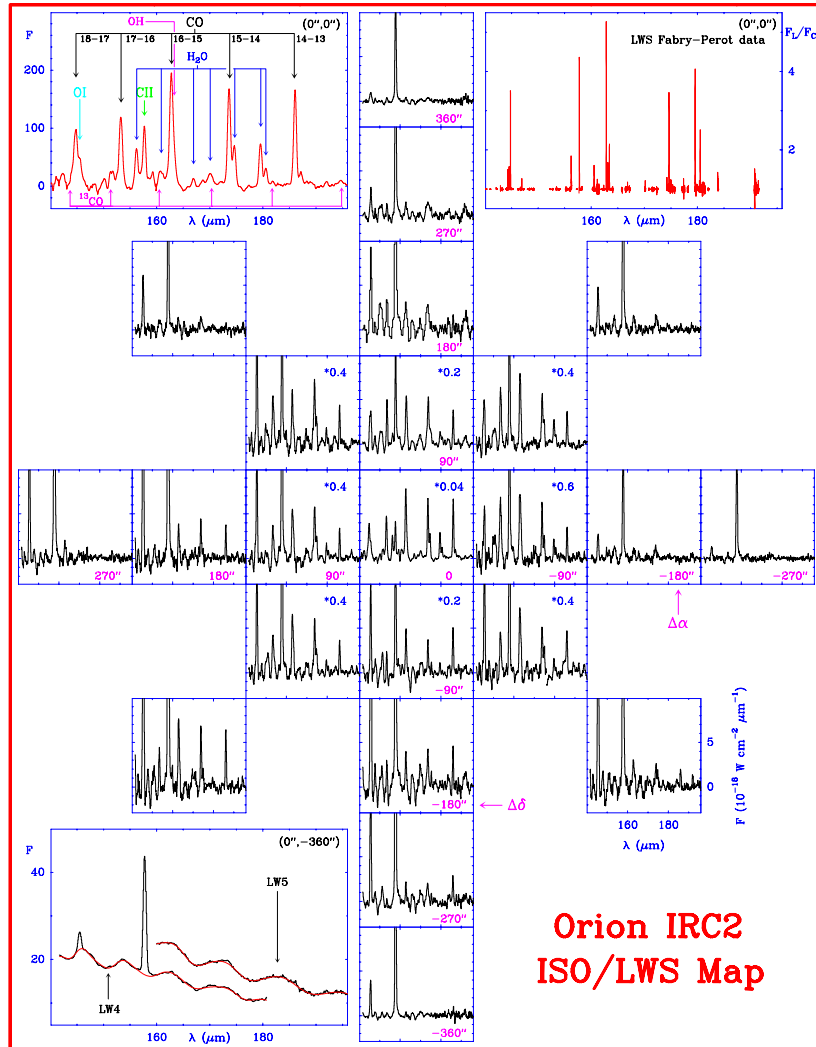


Figure 4. LWS raster of the Orion molecular cloud between 140 and 197 μm . Offsets, in arcseconds, are indicated in each box (in declination for the vertical strip and in right ascension for the horizontal one). Line identification are given in the zoom to the central position in the top-left panel. The CO data, including the LWS/FP data, have been presented and analyzed by Sempere et al. (2000).

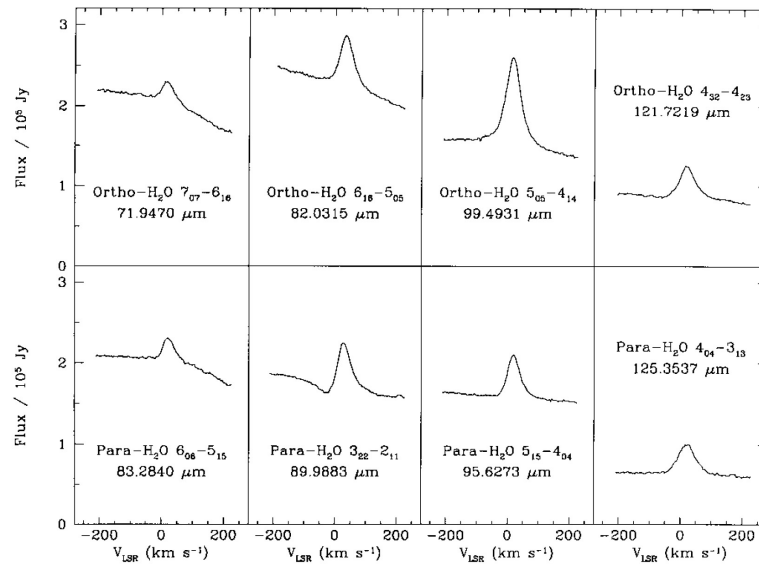
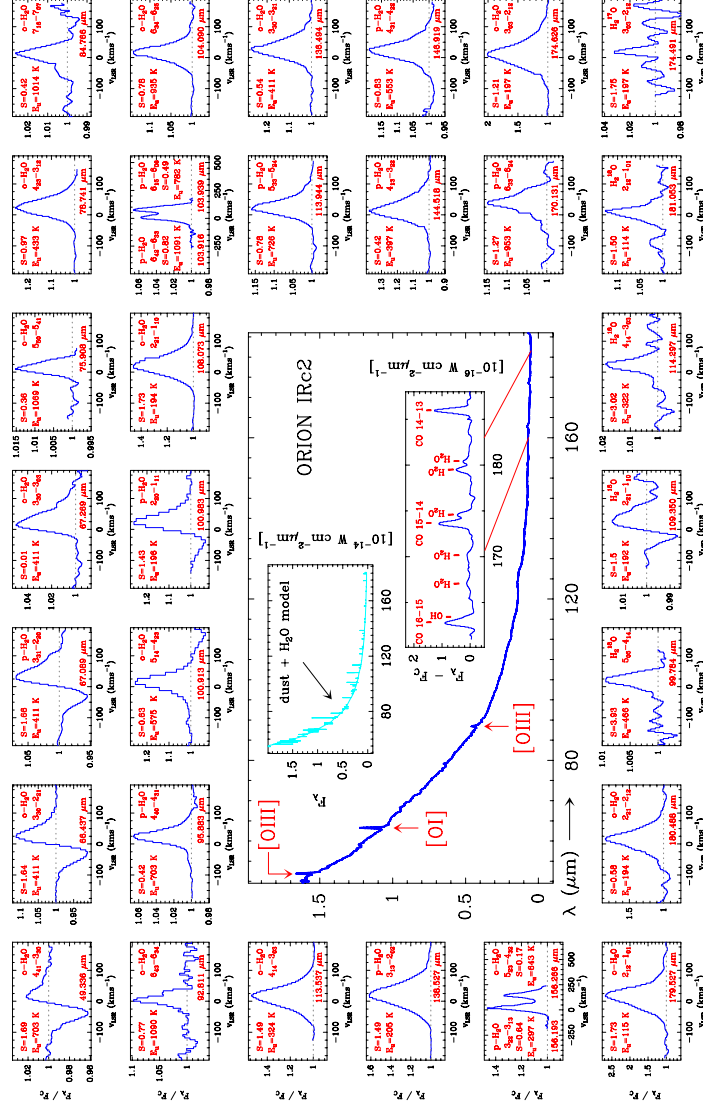


Figure 5. Water line profiles of the observed transitions in the direction of Orion (from Harwit et al., 1998).



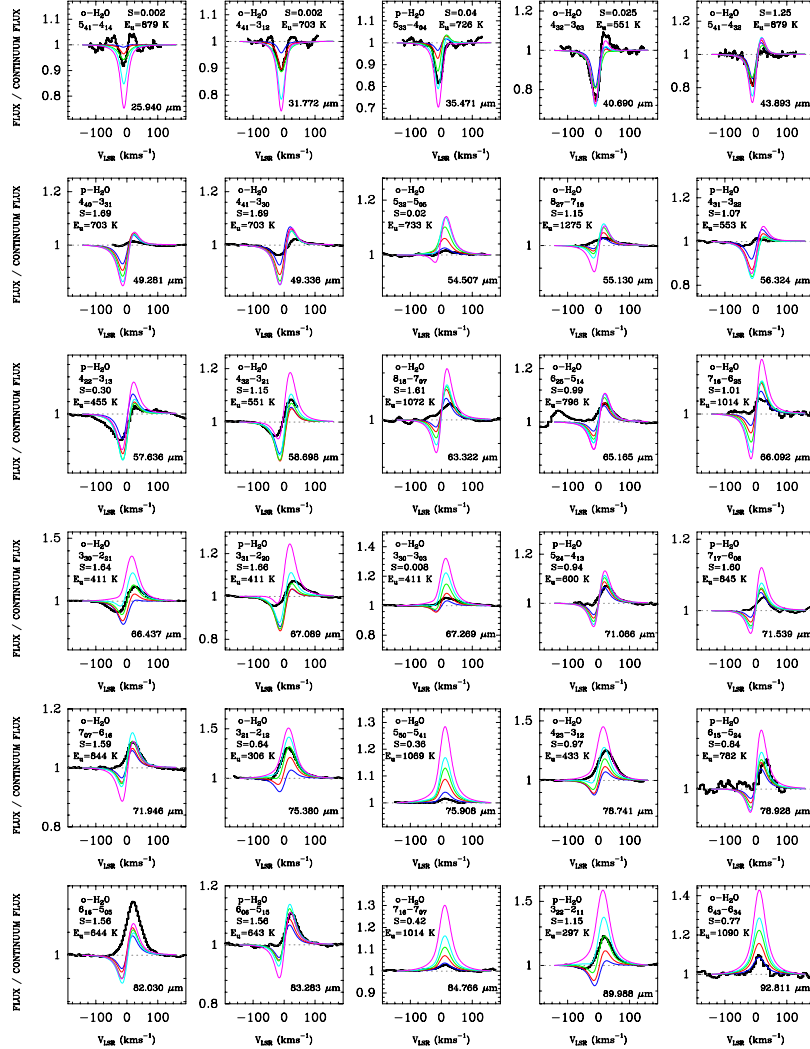


Figure 7. Some of the observed water lines (black thick line) together with the models discussed in the text which correspond to water abundances $(1, 2.5, 5, 10, 30) 10^{-5}$. See text for explanation of the effect of water abundance on the line profiles (from Cernicharo et al., 2005 and Daniel et al., 2005).

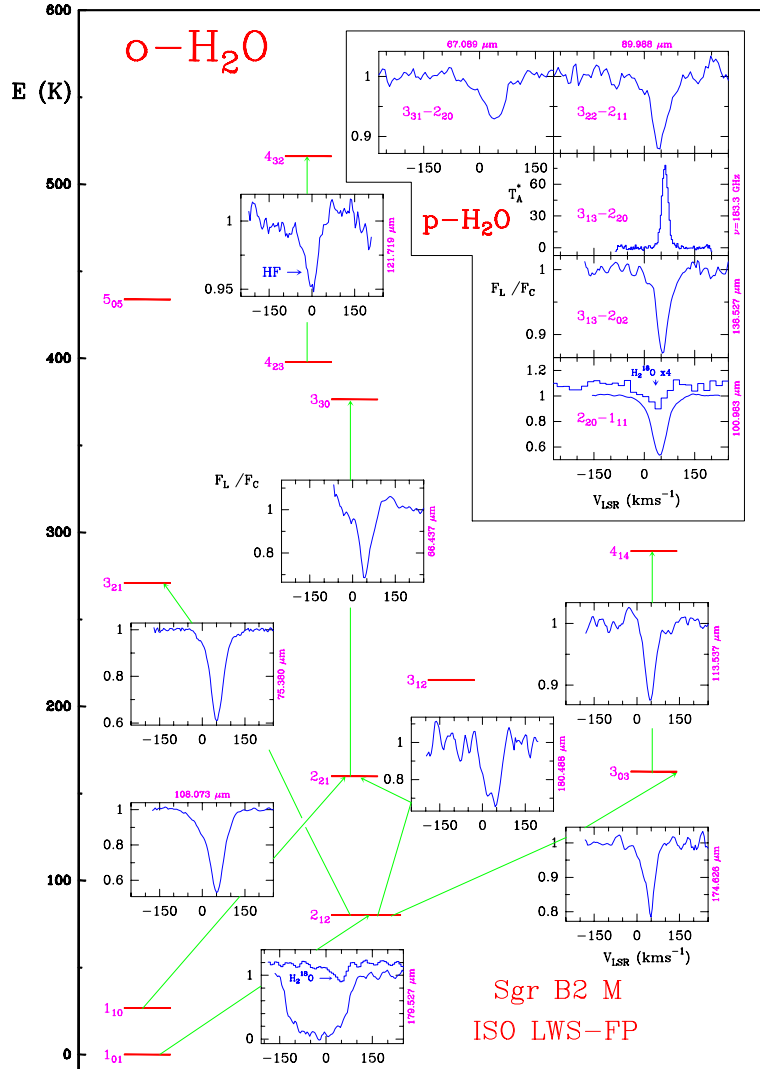


Figure 8. ISO/LWS/FP observations of H_2^{16}O and H_2^{18}O toward Sgr B2(M) and rotational energy diagram of ortho- H_2^{16}O . The ordinate scale corresponds to F_L/F_C and the abscissa to the wavelength in microns. All the far-IR water lines appear in absorption. The emission line corresponds to the $3_{13}-2_{20}$ maser transition of para- H_2^{16}O at 183 GHz (observed with the IRAM-30m telescope at Pico Veleta, Spain). From Cernicharo et al., (2005).

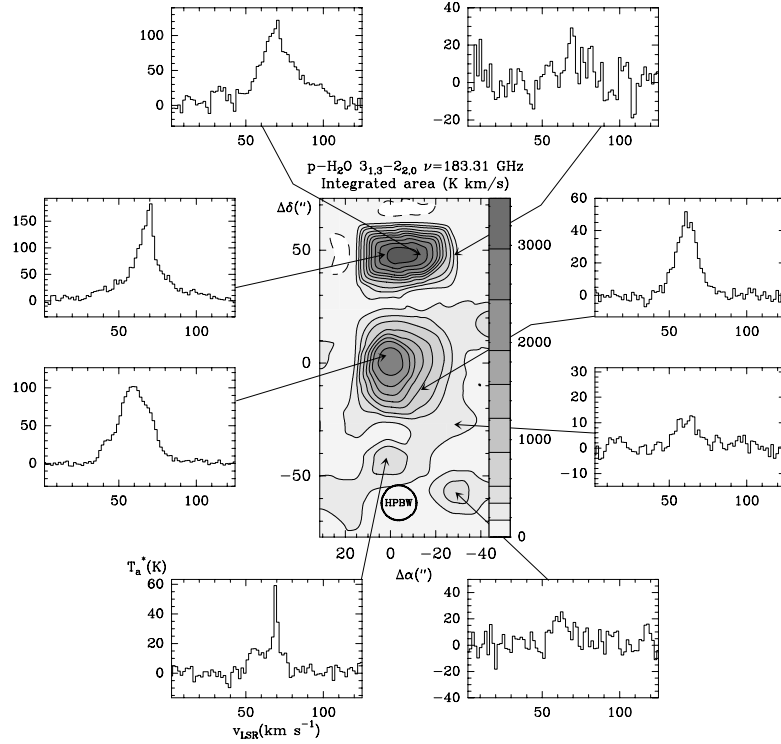


Figure 9. Map of the $3_{13}-2_{20}$ line of para- H_2^{16}O at 183 GHz around Sgr B2 main condensations. Contours in K km s^{-1} are indicated in the figure. Different line profiles at significant positions of the map are also shown. The intensity scale is in T_A^* and the abscissa is the LSR velocity in km s^{-1} . The map is centered at the position of Sgr B2(M) (from Cernicharo et al., 2005).

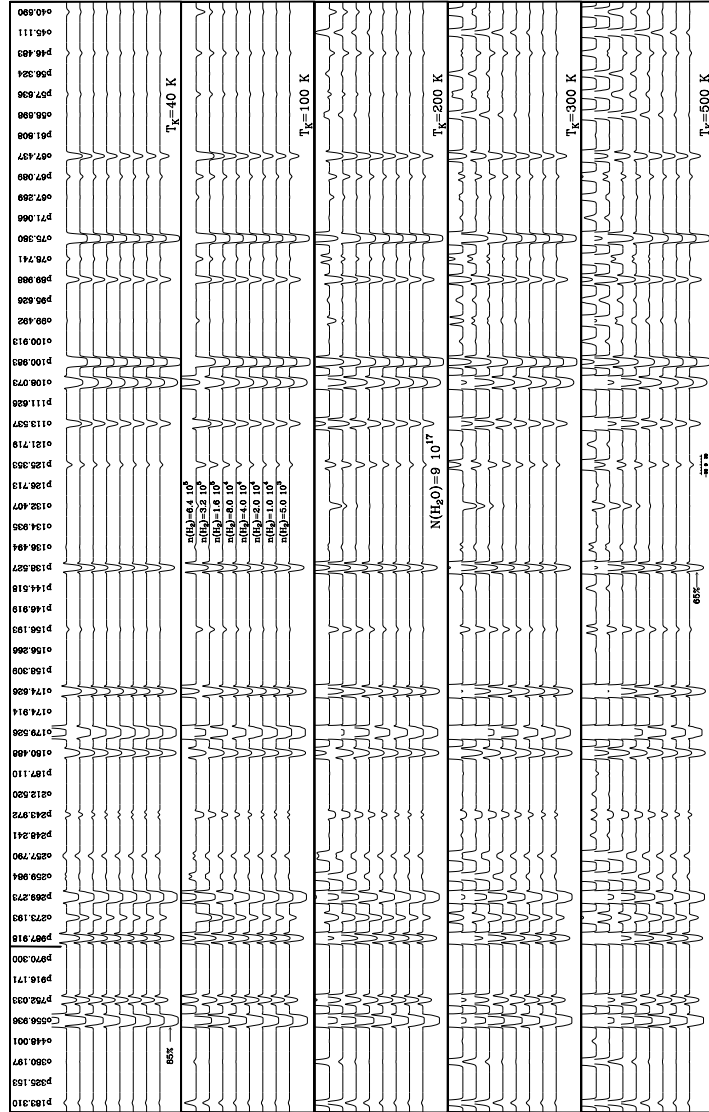


Figure 10. Results from selected nonlocal models of H_2O rotational lines in Sgr B2(M). The total H_2O column density is $9.0 \times 10^{17} \text{ cm}^{-2}$. Models for different kinetic temperatures (from 40 to 500 K) and H_2 densities (from 5.0×10^3 to $1.6 \times 10^5 \text{ cm}^{-3}$) are shown (from Cernicharo et al., 2005).

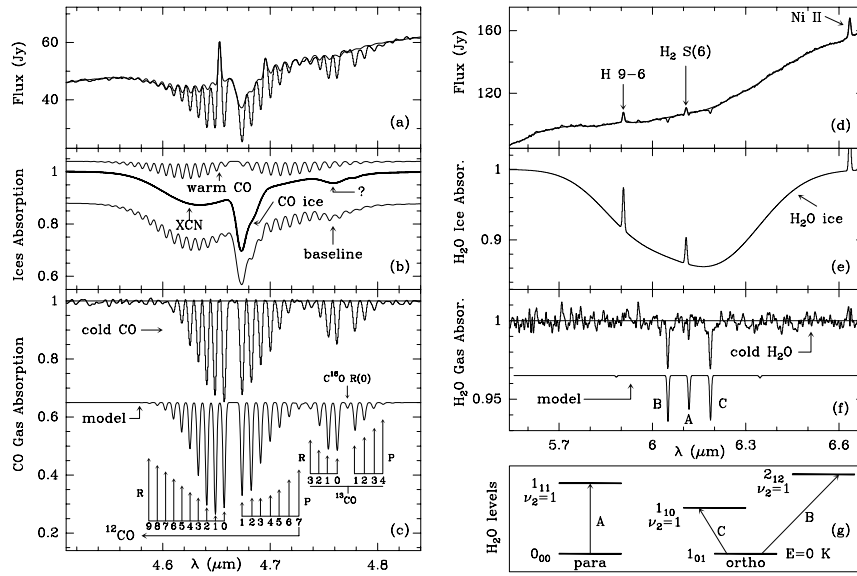


Figure 11. ISO/SWS spectra of the stretching mode of CO (a,b,c) and the bending mode of water vapor (d,e,f) in the direction of Sgr A*. Panels a and d show the observations and a model for the continuum (including ices); panels b and e show the contribution of the ices and of the warm CO; panels c and f show the normalized spectrum and model spectrum (shifted for clarity), and panel g shows the details of the ortho- and para-H₂O transitions (from Moneti, Cernicharo & Pardo 2000).

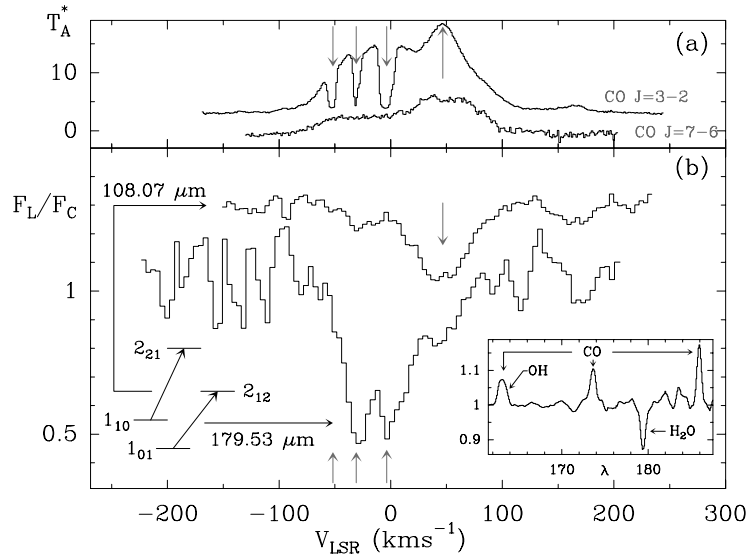


Figure 12. (a) $J=3-2$ and $J=7-6$ lines of CO observed at the CSO toward Sgr A*. The downward arrows indicate the central position of the cold gas absorption features. The upward arrows indicate the velocity of the Sgr A* molecular cloud. (b) LWS-FP spectra of the $2_{12}-1_{01}$ and $2_{21}-1_{10}$ lines of *o*-H₂O toward Sgr A*. The drawing at bottom left indicates the transition levels involved. The $1_{01}-2_{12}$ line shows three unresolved components at $v = 20, 5$ and 55 km s^{-1} while in the other transition only the 55 km s^{-1} feature is present. The inset panel shows the LWS-grating spectrum; the CO -warm gas- and H₂O lines are indicated. The upward arrows indicate the velocities of the cold absorbing gas and the downward arrow that of the Sgr A* molecular cloud (from Moneti, Cernicharo & Pardo, 2000)

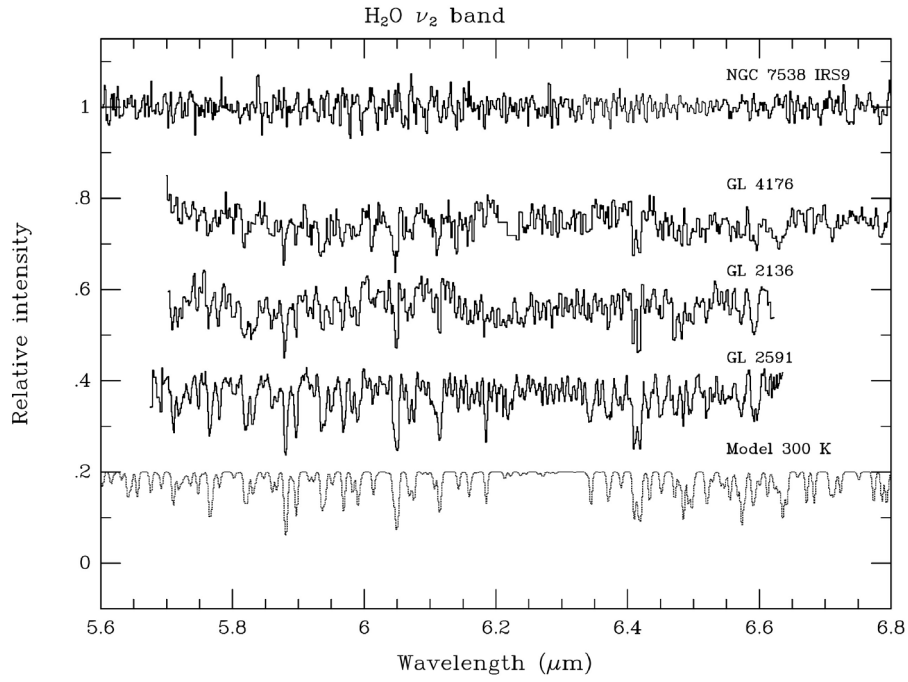


Figure 13. Normalized spectra of NGC7538 IRS9, GL4176, GL2136 and GL2591. A model H₂O spectrum for a column density of $2 \cdot 10^{18} \text{ cm}^{-2}$, $T_{\text{ex}}=300 \text{ K}$ and $\Delta v=5 \text{ km s}^{-1}$ is shown for comparison (from van Dishoeck and Helmich et al., 1996; see also Helmich et al., 1996b; see Boonman & van Dishoeck 2003 for observations of a large number of sources in the ν_2 mode of H₂O).

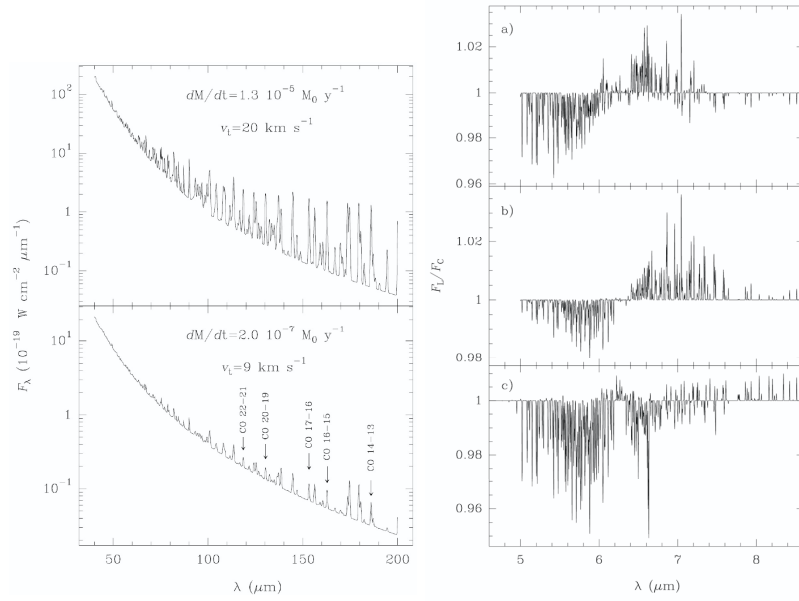


Figure 15. Left panel : Predicted ISO LWS spectrum of water vapor and CO for two models with mass loss rates and expansion velocities of $1.3 \cdot 10^{-5} M_{\odot} \text{ yr}^{-1}$ $V_{\text{exp}}=20 \text{ km s}^{-1}$ (upper subpanel) and $2 \cdot 10^{-7} M_{\odot} \text{ yr}^{-1}$ $V_{\text{exp}}=9 \text{ km s}^{-1}$ (lower subpanel). The water vapor and CO abundances are $2.7 \cdot 10^{-4}$ and $6 \cdot 10^{-4}$ respectively. The internal radius of the H_2O envelope is 10^{14} cm while the stellar radius is $3.7 \cdot 10^{13} \text{ cm}$. The source is placed at 500 pc and the models take into account the excitation of molecules to the bending mode. The lines of CO are indicated, all the remaining lines belong to H_2O . **Right panel :** Predicted ISO SWS spectrum of water vapor at $6 \mu\text{m}$ in the two models quoted above (panels (a) and (b)). Model c is similar to b except that the inner radius of the H_2O shell coincides with the stellar radius. The region between $r=R_*$ and $r=10^{14} \text{ cm}$ has $n(\text{H}_2)=2 \cdot 10^9 \text{ cm}^{-3}$ and $V_{\text{tur}}=5 \text{ km s}^{-1}$ (from González-Alfonso and Cernicharo 1999).

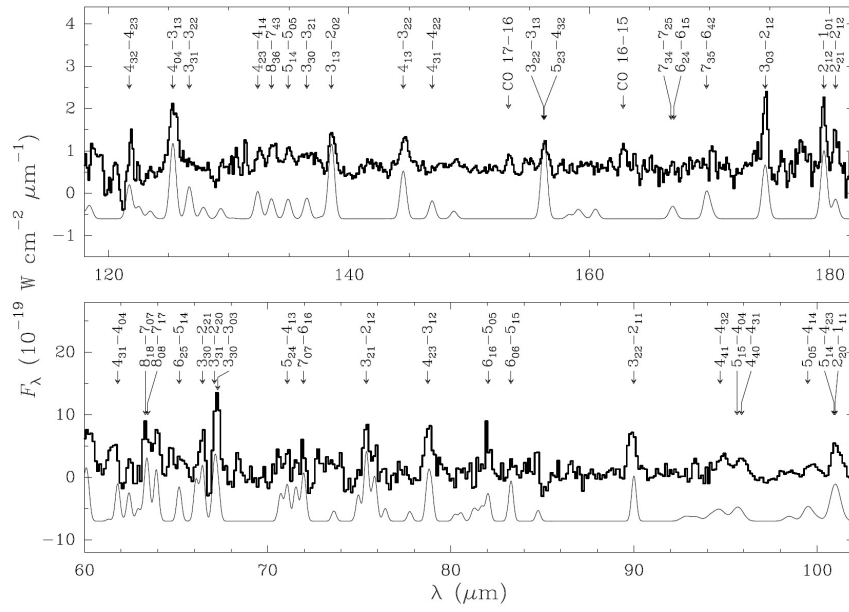


Figure 16. Continuum-subtracted LWS spectrum of W Hya together with the best fit model for water emission. The dominant transitions are labeled (from Barlow et al., 1996).

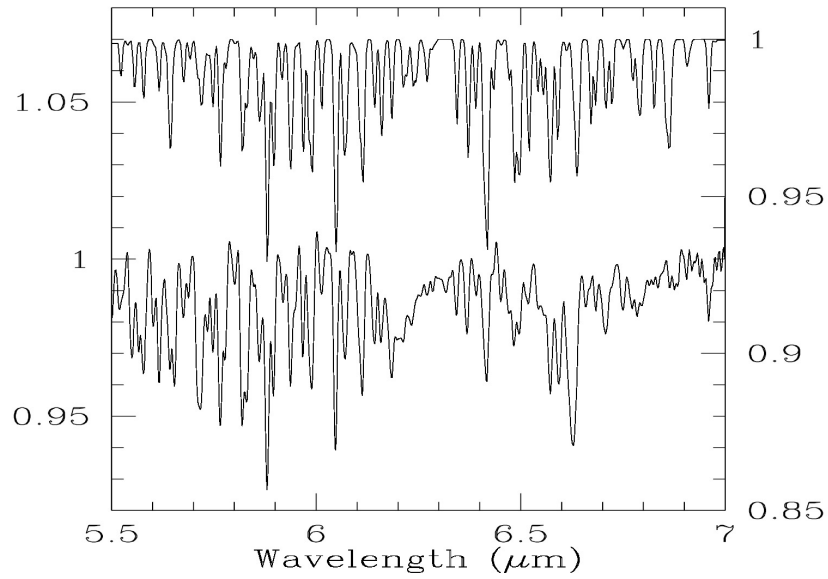


Figure 17. Continuum-divided spectrum of the ν_2 band of H_2O in NML Cyg (bottom). The modeled spectrum with $T_{\text{ex}}=100$ K and $N(\text{H}_2\text{O})=10^{19} \text{ cm}^{-2}$ is shown at the top (from Justtanont et al., 1996).

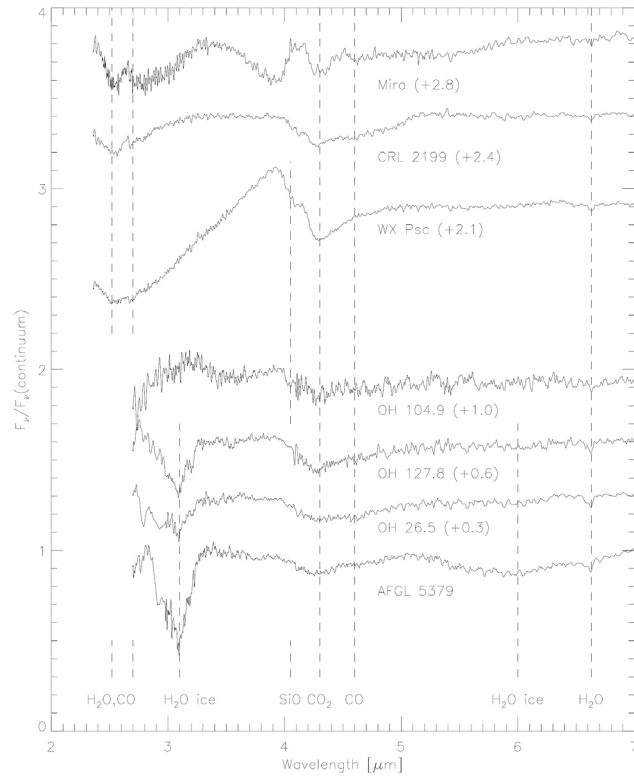


Figure 18. Continuum-divided spectra of several OH/IR stars in the 2-7 μm region. The central wavelengths of the absorption features due to H_2O (gaseous and ice phases), and of gaseous CO , CO_2 and SiO are indicated (from Sylvester et al., 1999).

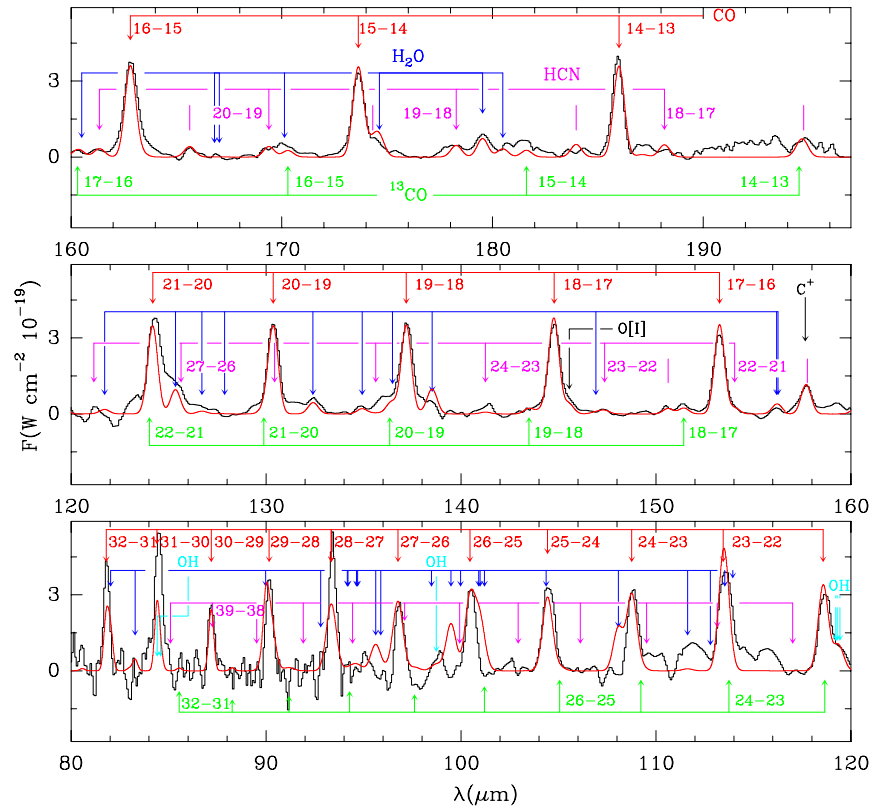


Figure 19. ISO/LWS Continuum-subtracted spectra of CRL618. The lines of CO, ^{13}CO , HCN, H_2O and OH are indicated by arrows, while those of HNC are indicated by vertical lines (from $J=22-11$ at $150.627\ \mu\text{m}$ to $J=17-16$ at $194.759\ \mu\text{m}$). The figure is from Herpin and Cernicharo (2000) and the result of their model is shown as a solid line.

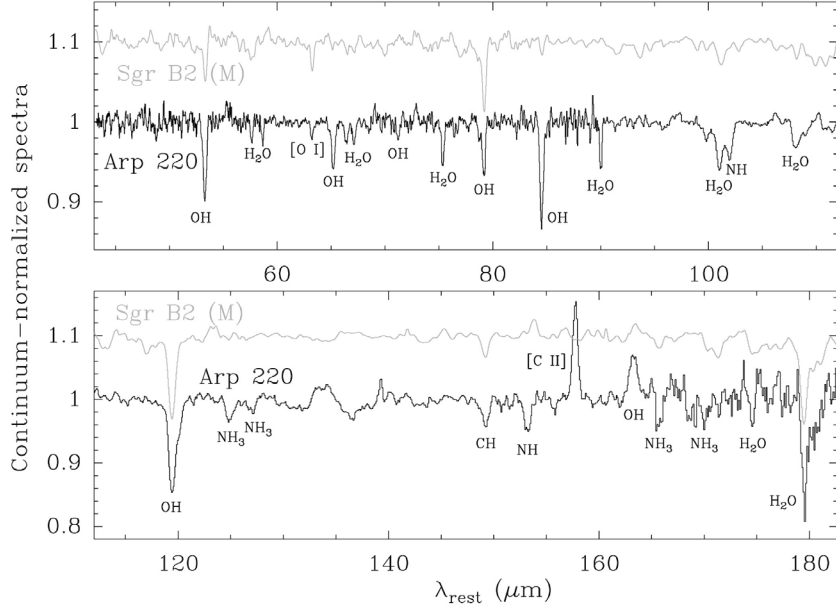


Figure 21. Continuum normalized spectra of SgrB2 (M) and Arp220. The main carriers of some line features are indicated. (from González-Alfonso et al., 2004).

In Arp220 González-Alfonso et al., (2004) have observed absorption in the lines of OH, H₂O, NH, NH₃ and CH in addition to [O I] at 63 μm and emission in the [C II] line at 158 μm . They have modeled the continuum and the emission/absorption of all observed features by using nonlocal radiative transfer codes. The continuum from 25 to 1300 μm corresponds to a nuclear region, optically thick in the far-infrared, with a size of 0.4'' and a dust temperature of 106 K surrounded by an extended region (2'') heated mainly through absorption of the nuclear infrared radiation. The OH column densities are high toward the nuclear region ($2\text{--}6 \cdot 10^{17} \text{ cm}^{-2}$) and in the extended region ($\approx 2 \cdot 10^{17} \text{ cm}^{-2}$) while the water column density is high toward the nucleus ($2\text{--}10 \cdot 10^{17} \text{ cm}^{-2}$) and lower in the extended region. The column densities in a halo that accounts for the absorption in the lowest lying lines are similar to what is found in the diffuse clouds toward the star-forming regions in the Sgr B2 molecular cloud in the neighborhood of the Galactic Center. One of the most surprising results from González-Alfonso et al., (2004) is the large column density needed to explain the observations of NH and NH₃ ($1.5 \cdot 10^{16} \text{ cm}^{-2}$ and $3 \cdot 10^{16} \text{ cm}^{-2}$, respectively) while NH₂, a molecule detected in Sgr B2 (M) by Goicoechea and Cernicharo (2001b), has a column density below $2 \cdot 10^5 \text{ cm}^{-2}$.

The excellent ISO spectrum of Arp220 makes it a reference template for understanding the dusty interstellar medium of ULIRGs. The model of

González-Alfonso et al., (2004) shows the important role of the dust photons in pumping the high-excitation lines of OH and H₂O, i.e., a similar situation to than that found in Sgr B2(M) (Goicoechea and Cernicharo, 2002). The modeling of water vapor and OH in Arp220 indicates the prominent role of PDR molecular chemistry in the extended region of Arp220, while chemistry in hot cores and shocks in the nucleus is also contributing to the observed abundance of H₂O.

Herschel, with its three instruments (HIFI, PACS and SPIRE), and its large telescope (3.5 m), will permit to observe the molecular content of more distant objects. The full frequency coverage provided by PACS and SPIRE will allow to make more detailed and sensitive studies of H₂O and OH, while HIFI will provide high spectral resolution of the line profiles of these molecules. It is worth noting that the H₂O models for water in Arp 220, and for sources in our galaxy, have required the simultaneous observation and modeling of other species, in particular OH and CO. Moreover, the use of galactic sources as templates as initial input for the interpretation of molecular extragalactic observations could be a mandatory step. Goicoechea, Martin-Pintado and Cernicharo (2005) have used Orion and Sgr B2 as templates to interpret the far-infrared spectra of NGC253 and NGC1064. Thanks to ISO, this information will be available when observing extragalactic sources with Herschel. It will be, without any doubt, the only way to interpret correctly the H₂O lines, which will provide important information on the chemistry and physical conditions of the gas.

5. Water in the Solar System

Water is ubiquitous in the Solar System. It is present

- as ice and liquid on the surface of the Earth;
- as ice and – presumably, in the past – as liquid on Mars;
- in various amounts in the atmospheres of most planets;
- as the main constituent of cometary ices;
- in primitive meteorites such as carbonaceous chondrites;
- as ice on numerous planetary satellites and – presumably – on trans-Neptunian objects (TNO);
- and even in the Sun's atmosphere.

Water is also a requisite for the apparition and evolution of life. It is thus important to know the cycle of water in the Solar System. Problems that are still open include:

- to which extent cometary (and TNO) ices are coming from unprocessed interstellar ice;
- what is the origin of water in the giant planets' atmospheres;
- to which extent did the infall of comets, asteroids and interstellar dust particles (IDPs) contributed to Earth (and Mars) water.

The contribution of ISO to cometary and planetary studies has also been reviewed by Crovisier (2000), Encrenaz (2000), Fouchet et al. (2004) and Müller et al. (2004).

5.1. COMETS

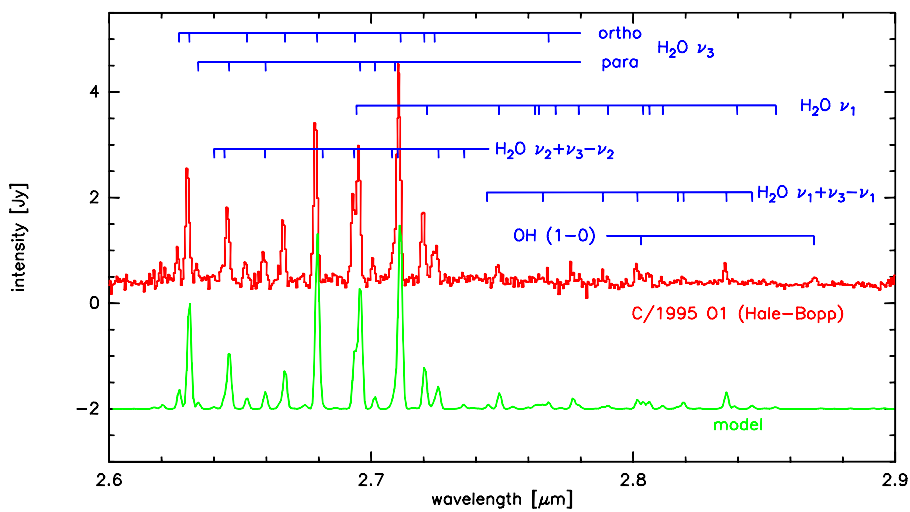


Figure 22. The SWS spectrum of water in the $2.7 \mu\text{m}$ region observed in comet C/1995 O1 (Hale-Bopp) on 27 September and 6 October at 2.8 AU from the Sun (top). Line assignments are indicated. The synthetic fluorescence spectrum which corresponds to the best fit to the data is shown at the bottom. It corresponds to $Q[\text{H}_2\text{O}] = 3.6 \times 10^{29} \text{ molecules s}^{-1}$, $T_{\text{rot}} = 28.5 \text{ K}$ and $T_{\text{spin}} = 28 \text{ K}$. Adapted from Crovisier et al. (1997a).

Water is the main constituent of cometary ices. Its sublimation governs cometary activity close to the Sun ($r \leq 4 \text{ AU}$). However, the direct observation of cometary water is very difficult from the ground, where only lines from infrared hot bands can be observed. The water ro-vibrational lines are emitted by fluorescence excited by solar radiation. Their measurement allows us to determine the water production rates in comets.

Water was best observed by ISO in the exceptionally bright comet C/1995 O1 (Hale-Bopp), as part of a target-of-opportunity program, in September–October 1996. The comet was then at $r = 2.8 \text{ AU}$ from the Sun and its water

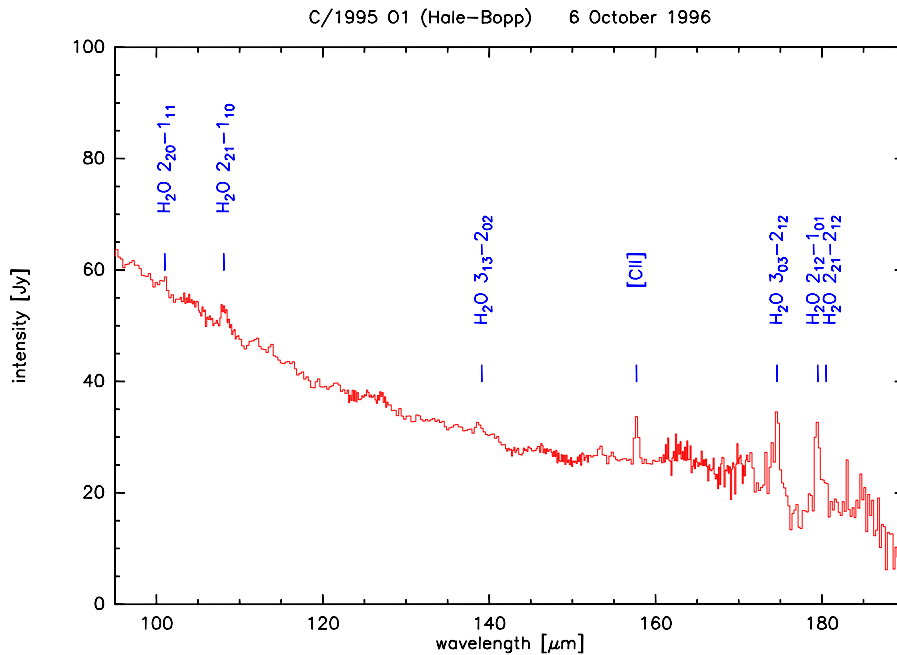


Figure 23. Several rotational lines of water observed in comet C/1995 O1 (Hale-Bopp) with the LWS. The ClI line is not cometary; it comes from the background (from Crovisier et al., 1999a).

production rate was 3.3×10^{29} molecules s^{-1} . The ν_1 , ν_3 and hot bands around $2.7 \mu\text{m}$ were resolved in rotation with the SWS (Fig. 22; Crovisier et al., 1997a, 1999b). The ν_2 band at $6.5 \mu\text{m}$ was also detected with the SWS, for the first time in a comet (Crovisier et al. 1997b). Several rotational lines ($2_{12}-1_{01}$ and $3_{03}-2_{12}$ around $180 \mu\text{m}$ and weaker ones) were observed with the LWS (Fig. 23). This was also the first detection of rotational lines of water in a comet, before the $1_{10}-1_{01}$ line at 557 GHz line could be observed by heterodyne techniques with the SWAS and Odin satellites.

In comet Hale-Bopp, water was only detected when the comet was at $r = 2.9$ and 3.9 AU . At farther distances (4.6 AU pre-perihelion and 4.9 AU post-perihelion), only CO and CO_2 (which are much more volatile species) were detected, with PHT-S. This shows the evolution between CO-dominated (at large r 's) and H_2O -dominated (at small r 's) regimes of sublimation of cometary ices.

ISO also observed H_2O in two short-period, Jupiter-family comets. In 103P/Hartley 2, which was observed close to its perihelion at $r = 1 \text{ AU}$, the water production rate was 1.2×10^{28} molecules s^{-1} (Colangeli et al. 1999; Crovisier et al. 1999a). In 22P/Kopff, observed in a less productive state after perihelion at $r = 1.9 \text{ AU}$, the water production rate was only 3.7×10^{27}

molecules s^{-1} and the water lines at $2.7 \mu\text{m}$ were just detected by the SWS (Crovisier et al. 1999a).

The SWS spectra obtained in the $2.6 \mu\text{m}$ region on comets Hale-Bopp and Hartley 2 allowed us to investigate the rotational distribution of water, and therefore its excitation conditions. Water excitation is governed by radiative excitation of the fundamental bands of vibration by the Sun IR radiation, collisions in the inner coma, and radiative trapping effects (Bockelée-Morvan 1987). On the other hand, the *kinetic* temperature of the coma is governed by the balance between radiative cooling (through emission of water rotational lines) and photolytic heating (principally through water photodissociation). In the field of view of the SWS, cometary water is partly relaxed to its lowest rotational levels. As predicted by modeling, the observed rotational temperatures of water are low: 28 K for Hale-Bopp, 20 K for Hartley 2, < 11 K for Kopff (Crovisier et al. 1997a, 1999a, 1999b).

Water exists in two nuclear-spin states according to the spins of its hydrogen atoms: ortho ($I = 1$) and para ($I = 0$). Conversions between the two states are forbidden, so that the ortho-to-para population ratio is linked to the temperature (spin temperature T_{spin}) of the last re-equilibration of water. The SWS spectra allowed us to determine T_{spin} of water in comets Hale-Bopp and Hartley 2. $T_{\text{spin}} = 28$ and 35 K were derived respectively for the two comets (Crovisier et al. 1997a, 1999a, 1999b). A similar value (29 K) was observed in the past for comet 1P/Halley (Mumma et al. 1993). The spin temperature of cometary ammonia (which is indirectly determined from the visible spectrum of NH_2 ; Kawakita et al. 2004) has also similar values (25–32 K).

These T_{spin} , all observed in a small range for comets of different orbits and different dynamical history, are still to be understood. It has been argued that T_{spin} could reflect the temperature of the grains where the molecules formed, but it seems hard to believe that the ortho-to-para ratio could be preserved over cosmological times without re-equilibration. T_{spin} could reflect the temperature of the inner nucleus ices. But then, one would expect different temperatures for comets with different orbits and history. It would be interesting to investigate by laboratory experiments if T_{spin} is preserved during the sublimation process, or if some fractionation occurs. It would also be interesting to compare the cometary water ortho-to-para ratio with those observed for interstellar water.

5.2. PLANETS AND SATELLITES

5.2.1. Mars

Water on Mars is now studied by a wealth of means. ISO also contributed to the observation of H_2O in Mars' atmosphere. Ro-vibrational absorption lines were observed in the 2.6 and $6.5 \mu\text{m}$ regions with the SWS, while many rotational lines were observed all over the 20 – 200 region with the SWS and

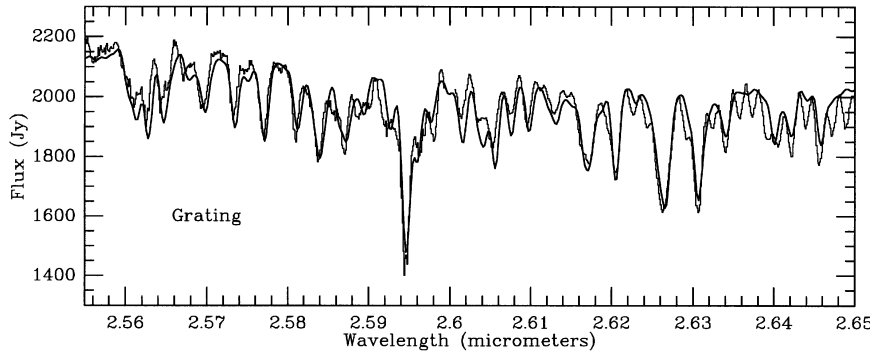


Figure 24. Lines of water in the 2.6 μm region of the spectrum of Mars, observed with the SWS grating. A modeled spectrum is superimposed (from Lellouch et al., 2000).

LWS (Fig. 24; Encrenaz et al. 1999; Burgdorf et al. 2000; Lellouch et al. 2000). From these observations, the mean water concentration at the ground was 4×10^{-4} at that time (31 July 1997) and saturation was reached at an altitude of 10 km. This corresponds to 15 μm of precipitable water.

5.2.2. Giant planets and Titan

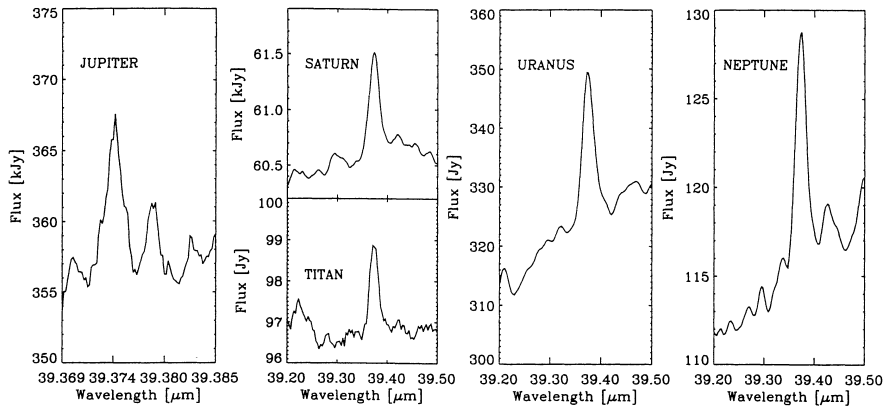


Figure 25. Examples of detections of H_2O lines in all four giant planets and Titan, with the SWS Fabry-Pérot (from Feuchtgruber et al., 1999).

An important result of ISO was the discovery of water in the stratospheres of the four giant planets and Titan. These detections are based upon water rotational lines observed in emission with the SWS and LWS, using the Fabry-Pérot (Fig. 25; Feuchtgruber et al. 1997, 1999; Coustenis et al. 1998; Lellouch et al. 2002; Encrenaz 2003). The disk-averaged water column den-

sities are observed in the range $\approx 10^{14} \text{ cm}^{-2}$ (Uranus, Neptune, Titan) to $\approx 2 \times 10^{15} \text{ cm}^{-2}$ (Jupiter, Saturn).

Because water condenses at the tropopause, its presence cannot be explained by an internal source of these objects. An external influx has to be invoked. This is the same for CO_2 , observed in the stratosphere of Jupiter, Saturn and Uranus.

5.3. THE CYCLE OF WATER IN THE SOLAR SYSTEM

Observations at infrared (ground-based and from ISO) and radio wavelengths point to the similarity between interstellar and cometary ices (Ehrenfreund et al. 1997; Bockelée-Morvan et al. 2000). This does not prove that comets accreted unprocessed interstellar ices, but rather suggests that similar chemical processes were at work in the primitive Solar Nebula and in interstellar clouds.

Impacts are an important phenomenon for the redistribution of water in the Solar System. Shock chemistry following the collisions of large bodies (planetesimals, comets, asteroids) will reshuffle most of the original molecular species. The oxygen compounds of the impactor could then lead to the formation of H_2O (and CO_2) in the post-impact chemistry. On the other hand, for infall of IDPs, the original molecules could be preserved. Icy IDPs could thus be an important source of water. Several studies have considered asteroids, comets and meteoroids as plausible sources of the water accreted by the Earth (e.g., Morbidelli et al. 2000). Martian water could have a similar origin.

The collision of comet Shoemaker-Levy 9 and Jupiter is a well documented case. Unfortunately, there is still ambiguity on the nature of the impactor (comet or asteroid?); its chemical nature could not be precisely characterized from pre-impact observations (Crovisier 1996). There is little doubt, however, that the chemical species observed after the impact result from shock chemistry, rather than coming from the impactor (Lellouch 1996).

In this context, three different sources have been invoked to explain the presence of oxygen species (water and carbon dioxide) discovered by ISO in giant planets (e.g., Encrenaz 2003; Lellouch et al. 2002; Fouchet et al. 2004):

- infall of IDPs;
- sputtering from icy rings and satellites; this is the preferred source for Saturn and Titan;
- impact of small bodies (comets and asteroids); this is certainly the case for Jupiter, for which the fall of comet Shoemaker-Levy 9 in 1994 provided the main source of oxygen.

6. Conclusions

Water has been found everywhere in space by ISO. The interpretation of the data is not straightforward but, nevertheless, we had for the first time the opportunity to study the role of water in the chemistry of all kind of objects in space, from solar system bodies to star forming regions, evolved stars and galaxies. Despite the limited spectral resolution of most water observations with ISO, the possibility to observe its full far and mid infrared spectrum has opened great possibilities in the interpretation of the data. Complex radiative transfer models able to treat the very large opacities of water have been developed, the chemistry of water on dust grains and gas phase has received an extraordinary and unique input from ISO, the presence of water in the upper layers of giant planets and their moons has told us about the chemistry of these objects, the detection of water in extragalactic sources could be used as a tracer of the physical and chemical processes prevailing in the nuclei of galaxies, etc.

Future missions like Herschel will benefit from the huge information ISO has provided on water vapor. The selection of water lines according to criteria of sensitivity to the physical parameters of the clouds, their interpretation and the prediction of the full spectrum of water in several clouds will be a mandatory step to prepare the Herschel mission. However, little new information will be obtained if collisional rates adapted to the temperatures of the clouds in the ISM and CSM are not available. Several aspects have to be improved for future water observations : we urgently need collisional rates for $\text{H}_2\text{O}-\text{H}_2$ at temperatures going from 10 to 2000 K (dark clouds to evolved stars). For AGB stars collisional rates between the ground and the bending mode are also necessary. These data have to be provided by physicists and chemists doing ab initio calculations or laboratory experiments. A very close collaboration between astronomers and the world of quantum chemistry is needed in order to promote these calculations and to be sure that we will get the maximum scientific output from Herschel when observing water in space.

Acknowledgements

We would like to thank J.R. Pardo, F. Daniel and J.R. Goicoechea for useful comments and suggestions and a critical reading of the manuscript. They have kindly provided several figures and calculations for this paper. J. Cernicharo thanks the Spanish Ministry of National Education (MEC) for funding support under grants AYA2003-2785, AYA2002-12125E, ESP2002-11650, AYA2002-10113-E, and ESP 2002-01627.

References

- Barlow M., et al.: 1996, The rich far-infrared water vapor spectrum of W Hya, *A&A*, **315**, L241–L244.
- Beckwith, S., Persson, S.E., Neugebauer, G., Becklin, E.E., 1978, *ApJ*, **223**, 484.
- Benedettini M., et al.: 2000, The ISO spectroscopic view of the HH24-26 region, *A&A*, **359**, 148–158.
- Blake G.A., Sutton E.C., Masson C.R., Phillips T.G., 1987, Molecular abundances in OMC-1 – The chemical composition of interstellar molecular clouds and the influence of massive star formation, *ApJ*, **315**, 621–645.
- Bockelée-Morvan, D.: 1987, A model for the excitation of water in comets, *A&A*, **181**, 169–181.
- Bockelée-Morvan, D., Lis, D.C., Wink, J.E., et al.: 2000, New molecules found in comet C/1995 O1 (Hale-Bopp): investigating the link between cometary and interstellar material, *A&A*, **353**, 1101–1114.
- Boonman A.M.S. & van Dishoeck E., 2003, Abundant gas-phase H₂O in absorption toward massive protostars, *A&A*, **403**, 1003–1010.
- Burgdorf, M.J., Encrenaz, T., Lellouch, E., et al.: 2000, ISO observations of Mars: an estimate of the water vapor vertical distribution and the surface emissivity, *Icarus*, **145**, 79–90.
- Ceccarelli C. et al., 1999a, The Far Infrared Spectrum of the Protostar IRAS16293-2422, *A&A*, **331**, 372–382
- Ceccarelli C. et al., 1999b, Water line emission in low-mass protostars, *A&A*, **342**, L21–L24
- Ceccarelli C. et al., 2002, ISO ammonia line absorption reveals a layer of hot gas veiling Sgr B2, *A&A*, **383**, 603–613
- Cernicharo, J. 1985, *ATM a program to compute atmospheric transmission between 0-1000 GHz*, IRAM internal report.
- Cernicharo, J. 1988, Ph.D. Thesis, Université de Paris VII.
- Cernicharo, J., Guélin M., 1987, The physical and chemical state of HCL2, *A&A*, **176**, 299–316.
- Cernicharo, J., Guélin M., Martin-Pintado J., Mauersberger R., 1989, A 200 km s⁻¹ molecular outflow in the protoplanetary nebula CRL618, *A&A*, **222**, L1–L4.
- Cernicharo, J., Thum, C., Hein, et al., 1990, Detection of 183 GHz water vapor maser emission from interstellar and circumstellar sources, *A&A*, **231**, L15–L17.
- Cernicharo, J., González-Alfonso, E., Alcolea, J. et al., 1994, Widespread water vapor emission in Orion, *ApJ*, **432**, L59–L62.
- Cernicharo, J., González-Alfonso, E., Bachiller, R. 1996a, Water emission at 183 GHz from HH7-11 and other low-mass star-forming regions, *A&A*, **305**, L5–L8.
- Cernicharo J. et al., 1996b, The ISO/LWS far Infrared Spectrum of IRC+10216, *A&A*, **315**, L201–L204.
- Cernicharo, J., Lim, T., Cox, et al., 1997a, Widespread water vapour absorption in SGR B2, *A&A*, **323**, L25.
- Cernicharo, J. 1997b, "The Far Infrared and Submillimeter Universe", 15-17 April 1997, Grenoble, France. *ESA SP-401*, page 91.
- Cernicharo, J., González-Alfonso, E., Lefloch, B., 1997c, "First Workshop on Analytical Spectroscopy", 6-8 October 1997a. *ESA SP-419*, page 23.
- Cernicharo J., X-Liu, González-Alfonso E., et al., 1997d, Discovery of Far-IR Pure Rotational Transitions of CH⁺ in NGC 7027, *ApJ*, **483**, L65
- Cernicharo J., 1998, Infrared Astrophysics in Space with ISO. From ISO to FIRST, *Ap&SS*, **263**, 175–192
- Cernicharo, J., González-Alfonso, E., et al., 1999a, in "The Universe as seen by ISO", Paris, 1999.

- Cernicharo, J., Pardo, E., Serabyn et al., 1999b, Physical Conditions in Shocked Regions of Orion from Ground-based Observations of H₂O, *ApJ*, **520**, L131-L134
- Cernicharo J., Goicoechea J.R., & Caux E., 2000, Far-infrared Detection of C₃ in Sagittarius B2 and IRC +10216, *ApJ*, **534**, L199-L202
- Cernicharo J. et al., 2001a, Infrared Space Observatory's discovery of C₄H₂, C₆H₂, and Benzene in CRL618, *ApJ*, **546**, L123-L126
- Cernicharo J. et al., 2001b, Methylpolyynes and Small Hydrocarbons in CRL618, *ApJ*, **546**, L127-L130
- Cernicharo J., 2004, The Polymerization of Acetylene, Hydrogen Cyanide, and Carbon Chains in the Neutral Layers of Carbon-rich Proto-planetary Nebulae *ApJ*, **608**, L41-L44
- Cernicharo J., Goicoechea J.R., Daniel F., et al., 2005, Far Infrared Water lines in Orion, *ApJ*, submitted
- Cheung A.C., Rank D.M., Townes C.H. et al., 1969, Detection of Water in Interstellar Regions by its Microwave Radiation, *Nature*, **221**, 626-629
- Clegg P. E. et al., 1996, The ISO Long-Wavelength Spectrometer, *A&A*, **315**, L38-L41
- Cohen M., Barlow M., Sylvester R.J. et al., 1999, Water Ice, Silicate, and PAH Emission Features in the ISO Spectrum of the C-rich Planetary Nebula CPD-56°8032, *ApJ*, **513**, L135-L138
- Colangeli, L., Epifani, E., Brucato, J. R. et al.: 1999, Infrared spectral observations of comet 103P/Hartley 2 by ISOPHOT, *A&A*, **343**, L87-L90.
- Comito C., Schilke P., Gerin M., et al., 2003, The line-of-sight distribution of water in the SgrB2 complex, *A&A*, **402**, 635-
- Coustonis, A., Salama, A., Lellouch, E., et al.: 1998, Evidence for water vapor in Titan's atmosphere from ISO/SWS data, *A&A*, **336**, L85-L89.
- Crovisier, J.: 1996, Observational constraints on the composition and nature of comet D/Shoemaker-Levy 9, in *The Collision of Comet Shoemaker-Levy 9 and Jupiter*, K.S. Noll, H.A. Weaver & P.D. Feldman (eds), Cambridge University Press, 31-54.
- Crovisier, J., Leech, K., Bockelée-Morvan, D. et al.: 1997a, The spectrum of comet Hale-Bopp (C/1995 O1) observed with the Infrared Space Observatory at 2.9 astronomical units from the Sun, *Science*, **275**, 1904-1907.
- Crovisier, J., Leech, K., Bockelée-Morvan, D., et al.: 1997b, The infrared spectrum of comet Hale-Bopp, in *First ISO Workshop on Analytical Spectroscopy*, A.M. Heras, K. Leech, N.R. Trams and M. Perry (eds), ESA SP-419, 137-140.
- Crovisier, J., Encrenaz, T., Lellouch, E., et al.: 1999a, ISO observations of short-period comets, in *The Universe as seen by ISO*, P. Cox and M.F. Kessler (eds), ESA SP-427, 161-164.
- Crovisier, J., Leech, K., Bockelée-Morvan, D., et al.: 1999b, The spectrum of comet Hale-Bopp as seen by ISO, in *The Universe as seen by ISO*, P. Cox and M.F. Kessler (eds), ESA SP-427, 137-140.
- Crovisier, J.: 2000, Observations of gas and dust in comets with the Infrared Space Observatory, in *Astrochemistry: From molecular Clouds to Planetary Systems* (IAU Symp. 197), Y.C. Mihn and E.F. van Dishoeck (eds), ASP, 461-470.
- Daniel F., Goicoechea J.R., Cernicharo J., et al., 2005, Modeling Water Vapor in Orion, *ApJ*, submitted
- de Graauw T. et al., 1996, Observing with the ISO Short-Wavelength Spectrometer, *A&A*, **315**, L49-L52
- Encrenaz, T., Feuchtgruber, H., Burgdorf, M., et al.: 1999, ISO observations of Mars: a determination of the water vapor vertical distribution, in *The Universe as seen by ISO*, P. Cox and M.F. Kessler (eds), ESA SP-427, 173-176.
- Encrenaz, T.: 2000, ISO Observations of Solar-System Objects, in *Infrared space astronomy, today and tomorrow* (École de Physique des Houches). F. Casoli, J. Lequeux, and F. David (eds), EDP Sciences, Paris, 89-150.

- Encrenaz, T.: 2003, ISO observations of the giant planets and Titan: what have we learnt? *P&SS*, **51**, 89–103.
- Ehrenfreund, P., d'Hendecourt, L., Dartois, E., et al.: 1997, ISO observations of interstellar ices and implications for comets, *Icarus*, **130**, 1–15.
- Feuchtgruber, H., Lellouch, E., de Graauw, T., et al.: 1997, External supply of oxygen to the atmospheres of giant planets, *Nature*, **389**, 159–162.
- Feuchtgruber, H., Lellouch, E., Encrenaz, T., et al.: 1999, Oxygen in the stratospheres of the giant planets and Titan, in *The Universe as seen by ISO*, P. Cox and M.F. Kessler (eds), ESA SP-427, 133–136.
- Fouchet T., Bézard B., Encrenaz T., : 2004, The planets observed by ISO, *this volume*.
- Gensheimer P.D., Mauersberger R., Wilson T.L., 1996, Water in galactic hot cores, *A&A*, **314**, 281–294.
- Genzel R., and Stutzki J., 1989, The Orion Molecular Cloud and star-forming region, *ARAA*, **27**, 41–85
- Genzel R., Reid M.J., Moran J.M., Downes D., 1981, Proper motions and distances of H₂O maser sources. I – The outflow in Orion-KL, *ApJ*, **244**, 884–902
- Gibb E.L., Whittet D.C.B., Bougert A.C.A., Tielens A.G.G.M., 2004, Interstellar Ice : The ISO legacy, *ApJSS*, **151**, 35–73
- Goicoechea J.R., Cernicharo J., 2001a, Far-Infrared Detection of H₃O⁺ in Sagittarius B2, *ApJ*, **554**, L213–L215
- Goicoechea J.R., Cernicharo J., 2001b, Spectroscopy of key Molecular Species in the Far-Infrared, in *The Promise of FIRST*, edd. G.L. Pilbratt, J. Cernicharo, A.M. heras, T. Prusti & R. Harris, *ESA SP-460; Noordwijk: ESA/ESTEC*, 413–416.
- Goicoechea J.R., Cernicharo J., 2002, Far-Infrared OH Fluorescent Emission in Sagittarius B2, *ApJ*, **576**, L77–L80
- Goicoechea J.R., Rodríguez-Fernández N.J., Cernicharo J., 2004, The Far-Infrared Spectrum of the Sagittarius B2 Region: Extended Molecular Absorption, Photodissociation, and Photoionization, *ApJ*, **600**, 214–233
- Goicoechea J.R., Martín-Pintado J., Cernicharo J., 2005, OH Rotational Lines as a Diagnostic of the Warm Neutral Gas in Galaxies, *ApJ*, **619**, 291–296.
- González-Alfonso E., Cernicharo J., 1993, HCN Hyperfine Anomalies, *A&A*, **279**, 506–520
- González-Alfonso E., Cernicharo J., Bachiller R., Fuente A., 1995, 183 GHz water emission in W 49N, *A&A*, 293, L9.
- González-Alfonso E., Cernicharo J., 1997, Explanation of ²⁹SiO, ³⁰SiO and high-*v* ²⁸SiO maser emission, *A&A*, **322**, 938–942
- González-Alfonso, E., Cernicharo, J., Alcolea, J., Orlandi, M.A. 1998a, Water vapor in circumstellar envelopes, *A&A*, 334, 1016.
- González-Alfonso E., Cernicharo J., van Dishoeck E.F. et al., 1998b, Radiative Transfer Models of Emission and Absorption in the H₂O 6 Micron Vibration-Rotation Band Toward Orion-BN-KL, *ApJ*, 502, L169.
- González-Alfonso, E. and Cernicharo, J., 1999, The Water Vapor Abundance in Circumstellar Envelopes, *ApJ*, **525**, 845–862.
- González-Alfonso E., Wright C.M., Cernicharo J. et al., 2002, The Far-Infrared Spectrum of Arp 220, *A&A*, **386**, 1074–1102.
- González-Alfonso E., Smith H.A., Fischer J., Cernicharo J., 2004, The Far-Infrared Spectrum of Arp 220, *ApJ*, **613**, 247–261
- Harwit, M. Neufeld, D.A., Melnick, G.J., Kaufman, M.J., 1998, Thermal Water Vapor Emission from shocked regions in Orion, *ApJ*, **497**, L105–L108
- Helmich F.P., van Dishoeck E.F., Jansen D.J., 1996a, The excitation and abundance of HDO toward W3(OH)/(H₂O), *A&A*, **313**, 657–663

- Helmich F.P., van Dishoeck E.F., Black J.H. et al., 1996b, Detection of hot, abundant water toward AFGL 2591, *A&A*, **315**, L173–L176
- Herpin F. & Cernicharo J., 2000, O-bearing Molecules in Carbon-Rich Proto-Planetary Objects, *ApJ*, **530**, L129–L132
- Herpin F., Goicoechea J.R., Pardo J.R., Cernicharo J., 2002, Chemical Evolution of the Circumstellar Envelopes of Carbon-rich post-AGB Objects, *ApJ*, **577**, 961–973
- Hjalmarson A. et al., 2003, Highlights from the first year of Odin observations, *A&A*, **402**, L39–L42
- Hüttemeister S., Wilson T. L., Mauersberger R., Lemme C., Dahmen G., Henkel C. 1995, A multilevel study of ammonia in star-forming regions. 6: The envelope of Sagittarius B2 *A&A*, **294**, 667–676
- Jacq T., Jewell P.R., Henkel C., Walmsley C.M., Baudry A., 1988, $H_2^{18}O$ in hot dense molecular cloud cores, *A&A*, **199**, L5
- Jacq T., Walmsley C.M., Henkel C., et al., 1990, Deuterated water and ammonia in hot cores, *A&A*, **228**, 447
- Justtanont, K., de Jong, T., Helmich, F. P., et al., 1996, The ISO-SWS spectrum of NML Cyg, *A&A*, **315**, L217–L220
- Justtanont K., de Jong T., Tielens A.G.G.M, et al., 2004, Deuterated water and ammonia in hot cores, *A&A*, **417**, 625–635
- Kawakita, H., Watanabe, J., Furusho, R., et al.: 2004, Spin temperatures of ammonia and water molecules in comets. *ApJ*, **601**, 1152–1158.
- Kessler M.F. et al., 1996, The Infrared Space Observatory (ISO) mission, *A&A*, **315**, L27–L30
- Lellouch, E.: 1996, Chemistry induced by the impacts: observations, in *The Collision of Comet Shoemaker-Levy 9 and Jupiter*, K.S. Noll, H.A. Weaver & P.D. Feldman, (eds), Cambridge University Press, 213–242.
- Lellouch, E., Encrenaz, T., de Graauw, T., et al.: 2000, The 2.4–45 μ m spectrum of Mars observed with the Infrared Space observatory, *P&SS*, **48**, 1393–1405.
- Lellouch, E., Bézard, B., Moses, J. I.: 2002, The origin of water vapor and carbon dioxide in Jupiter's stratosphere, *Icarus*, **159**, 112–131.
- Lis, D.C. & Goldsmith, P.F. 1990, Modeling of the continuum and molecular line emission from the Sagittarius B2 molecular cloud, *ApJ*, **356**, 195–210
- Liseau R., Ceccarelli C., Larsson B., et al., 1996, Thermal H_2O emission from the Herbig-Haro flow HH54, *A&A*, **315**, L181–L184
- Maret S., Ceccarelli C., Caux E., Tielens A.G.G.M., Castets A., 2002, Water emission in NGC1333-IRAS4 : The physical structure of the envelope, *A&A*, **395**, 573–585
- Melnick, G. J., et al., 2000, The Submillimeter Wave Astronomy Satellite: Science Objectives and Instrument Description, *ApJ*, **539**, L77–L80
- Melnick G.J., Neufeld D.A, Ford K.E.S et al., 2001, Discovery of water vapour around IRC+10216 as evidence for comets orbiting another star, *Nature*, **412**, 160–163
- Menten K., & Melnick G.J. 1991, 321 GHz submillimeter water masers around evolved stars, *ApJ*, **377**, 647–656
- Menten, K.L, Melnick, G.J., Phillips, T.G. 1990a, Submillimeter water masers, *ApJ*, **350**, L41–L44.
- Menten K.L, Melnick G.J., Phillips T.G., Neufeld D.A., 1990b, A new submillimeter water maser transition at 325 GHz, *ApJ*, **363**, L27–L30.
- Molster T.J., et al., 2001, The Complete ISO Spectrum of NGC6302, *A&A*, **372**, 165–172
- Moneti A., Cernicharo J., Pardo J.R., 2000, Cold H_2O and CO Ice and Gas toward the Galactic Center, *ApJ*, **549**, L203–L206
- Morbidelli, A., Chambers, J., Lunine, J.I., et al.: 2000, Source regions and timescales for the delivery of water to Earth, *Meteoritics Planet. Sci.*, **35**, 1309–1320.

- Moro-Martin A., Noriega-Crespo A., Molinari S., Testi L., Cernicharo J., Sargent A., 2001, Infrared and Millimetric Study of the Young Outflow Cepheus E, *ApJ*, **555**, 146–159
- Müller, T.G., Abrahám, P., and Crovisier, J.: 2004, Comets, asteroids and zodiacal light as seen by ISO, *this volume*.
- Mumma, M.J., Weissman, P.R., and Stern, S.A.: 1993, Comets and the origin of the solar system: reading the Rosetta stone, in *Protostars and Planets III*, E.H. Levy & J.I. Lunine (eds), Univ. Arizona Press, Tucson, 1177–1252.
- Neufeld D.A., Kaufman M.J., 1993, Radiative Cooling of Warm Molecular Gas, *ApJ*, 418, 263
- Neufeld, D.A.; Lepp, S., & Melnick, G.J. 1995, Thermal Balance in Dense Molecular Clouds: Radiative Cooling Rates and Emission-Line Luminosities, *ApJ*, 100, 132
- Neufeld D.A., Chen W., Melnick G.J. et al., 1996, *A&A*, 315, L237.
- Neufeld, D.A., Zmuidzinas, J., Schilke, P., & Phillips, T.G. 1997, Discovery of Interstellar Hydrogen Fluoride, *ApJ*, **488**, L141–L144
- Neufeld D.A., Feuchtgruber H., Harwit M., Melnick G., 1999, ISO observations of far-Infrared rotational emission lines of H₂O toward VY CMa, *ApJ*, **517**, L147–L150
- Neufeld, D.A., Ashby, M.L.N., Bergin, E.A., et al., 2000, Observations of Absorption by Water Vapor toward Sagittarius B2, *ApJ*, **539**, L111–L114
- Neufeld, D.A., Bergin, E.A.; Melnick, G.J., Goldsmith, P.F. 2003, Submillimeter Wave Astronomy Satellite Mapping Observations of Water Vapor around Sagittarius B2, *ApJ*, **590**, 882–994
- Nisini B., Lorenzetti D., Cohen M., et al., 1996, LWS-spectroscopy of Herbig Haro objects and molecular outflows in the Cha II dark cloud, *A&A*, **315**, L321–L324
- Nisini B., Benedettini M., Giannini T. et al., 2000, Far Infrared mapping of the gas cooling along the L1448 outflow, *A&A*, **360**, 297–310
- Nisini B., Giannini T., Lorenzetti D., 2002, Evolution in the Far-Infrared Spectra of low Mass Young Embedded Sources, *ApJ*, **574**, 246–257
- Nisini B., 2003, Mid and Far Infrared Observations of Protostellar jets, *Ap&SS*, **287**, 207–212
- Omont A., Moseley S.H., Forveille T., et al., 1990, Observations of 40–70 micron bands of ice in IRAS 09371+1212 and other stars, *ApJ*, **355**, L27–L30
- Pardo, J.R. 1996, Ph.D. Thesis, Université Pierre et Marie Curie, Paris, France
- Pardo J.R., Cernicharo J., Serabyn G., 2001a, Atmospheric Transmission at Microwaves (ATM) : an improved model for mm/submm Applications, *IEEE Transactions on Antennas and Propagation*, **49**, 1683-1694
- Pardo J.R., Cernicharo J., Herpin F., et al., 2001b, Deuterium Enhancement in Water toward Orion IRC2 Deduced from HDO Lines above 800 GHz, *ApJ*, **562**, 799–803
- Phillips T.G., Kwan J., and Huggins P.J. 1980, in *IAU Symposium 87 : Interstellar Molecules*, ed. B.H. Andrew (Dordrecht: Reidel), p 21.
- Phillips T.G., van Dishoeck E., Keene J., 1992, Interstellar H₃O⁺ and its relation to the O₂ and H₂O abundances, *ApJ*, **399**, 533–550
- Plume R., Kaufman M.J., Neufeld D.A., et al., 2004, Water Absorption from Line-of-Sight Clouds Toward W49A, *ApJ*, **605**, 247–258
- Polehampton E.T., Baluteau J.P., Ceccarelli C., Swinyard B.M., Caux E., 2002, Detection of HD in emission towards Sagittarius B2, *A&A*, **388**, L44–L47
- Polehampton E.T., Menten K., Brunken S., Winnewise G., Baluteau J.P., 2005, Far-infrared detection of methylene, *A&A*, **431**, 203–213
- Saraceno P., Ceccarelli C., Clegg P., et al., 1996, LWS Observations of the bright rimmed globule IC1396N, *A&A*, 315, L293–L296
- Sempere M.J., Cernicharo J, Lefloch B., et al., 2000, Extended Far-Infrared CO Emission in the OMC-1 core of Orion, *ApJ*, **530**, L123–L126

- Snell R.L., Howe J.E., Ashby M.L.N., et al., 2000, Water Abundance in Molecular Cloud Cores, *ApJ*, **539**, L101–L105
- Spoon H.W.W., Keane J.V., Tielens A.G.G.M., et al., 2002, Water Abundance in Molecular Cloud Cores, *A&A*, **385**, 1022–1041
- Sylvester R.J., Kemper F., Barlow M.J., et al., 1999, 2.4–197 μm spectroscopy of OH/IR stars: the IR characteristics of circumstellar dust in O-rich environments, *A&A*, **352**, 587–599
- Truong-Bach R.J. et al., 1999, H₂O from R Cas: ISO LWS-SWS observations and detailed modeling, *A&A*, **345**, 925–935
- van der Tak et al., 2005, Benchmark problems for water radiative transfer, Proceedings of the dusty and molecular universe: a prelude to Herschel and ALMA, 27–29 October 2004, Paris, France. Ed. by A. Wilson. ESA SP-577, Noordwijk, Netherlands: ESA Publications Division, ISBN 92-9092-855-7, 2005, p. 431 - 432
- van Dishoeck E., Helmich F., 1996, Infrared absorption of H₂O toward massive young stars, *A&A*, **315**, L177–L180
- van Dishoeck, E., Wright, C.M., Cernicharo, J. et al., 1998, The ISO-SWS 2.4–45.2 Micron Spectrum Toward Orion IRC2, *ApJ*, **502**, L173–L176.
- van Dishoeck E., 2004, ISO SPECTROSCOPY OF GAS AND DUST: From Molecular Clouds to Protoplanetary Disks, *ARA&A*, **42**, 119–167
- Waters, J.W., Gustincic, J.J., Kakar, et al., 1980, Observations of interstellar H₂O emission at 183 GHz, *ApJ*, **235**, 57–62.
- Wright C.M., van Dishoeck E.F., Black J.H., et al., 2000, ISO-SWS observations of pure rotational H₂O absorption lines toward Orion-IRC2, *A&A*, **358**, 689–700.
- Zmuidzinas J., Blake G.A., Carlstrom J., et al., 1995, “Submillimeter spectroscopy of interstellar hydrides”, ASP Conference Series, Vol. 73. Ed. M.R. Haas, J.A. Davidson and E.F. Erickson., p. 33
- Zubko V., et al., 2004, Observations of water vapor outflow from NML Cygnus, *ApJ*, **610**, 427–435.

